HIGHER MOMENTS OF MULTIPLICITY DISTRIBUTION IN HEAVY ION COLLISION

Anjali Krishnan

A dissertation submitted for the partial fulfilment
of BS-MS dual degree in Science

Indian Institute of Science Education and Research Mohali

April 2017

Certificate of Examination

This is to certify that the dissertation titled **"Higher moments of multiplicity distribution in heavy ion collision"** submitted by **Anjali Krishnan** (Reg. No. MS12054) for the partial fulfillment of BS-MS dual degree programme of the Institute, has been examined by the thesis committee duly appointed by the Institute. The committee finds the work done by the candidate satisfactory and recommends that the report be accepted.

Dr. Ketan Patel | Dr. Sanjeev Kumar | Dr. Satyajit Jena (Supervisor)

Dated: 21.04.2017

Declaration

The work presented in this dissertation has been carried out by me under the guidance of Dr. Satyajit Jena at the Indian Institute of Science Education and Research Mohali.

This work has not been submitted in part or in full for a degree, a diploma, or a fellowship to any other university or institute. Whenever contributions of others are involved, every effort is made to indicate this clearly, with due acknowledgement of collaborative research and discussions. This thesis is a bonafide record of original work done by me and all sources listed within have been detailed in the bibliography.

Anjali Krishnan
(Candidate)

Dated: April 21, 2017

In my capacity as the supervisor of the candidate's project work, I certify that the above statements by the candidate are true to the best of my knowledge.

Dr. Satyajit Jena
(Supervisor)

Acknowledgement

First and foremost, I would like to thank my thesis supervisor Dr. Satyajit Jena, without whose help and supervision, this thesis would have never been possible. The discussions that I had with him has enhanced my capabilities as a researcher.

I would also like to thank my thesis committee members Dr. Ketan Patel and Dr. Sanjeev Kumar for their valuable suggestions and criticism of my work.

I owe my deepest gratitude to Rohit Gupta for helping me with the discussions and data collection. I would like to mention my heartiest gratitude to all my lab members.

I would like to thank IISER Mohali Library facility. I am highly grateful to the Deputy librarian, Dr. Vishaki, and Library Information Assistant, Mr. Shameer K. K. for their promptness and assistance.

I would like to thank all my friends for supporting and helping me during the entire period of the project. I am thankful also to my seniors for their useful advice and help. I would like to acknowledge the moral support and encouragement, that I have received from my parents and brother.

Finally, I am thankful to IISER Mohali for providing me infrastructure and Computer Centre for all the technical support. I would like to acknowledge DST INSPIRE, Government of India for the financial support.

Anjali Krishnan
MS12054
IISER Mohali.

List of Figures

Contents

Abstract

According to Big-Bang theory, at the earliest of its expansion, universe existed as QGP. As it cools down, the deconfined-confined phase transition occurred and hadrons were formed. Study about these kind of a stage can lead us to understand the early stages of universe formation. The transformation of matter at higher enough energies, from nucleons to constituent quarks and gluons had been very interesting and equally very challenging.

Even though the energy scale is quite challenging, in heavy ion collisions we were trying to create a similar system and studying various properties. Since the multiplicity of produced particles is an important quantity to characterize the evolving system and its event to event fluctuation may provide a distinct signal of the phase transition from hadron gas to QGP. Higher moments of a distribution can give important information about the asymmetry of the system. Considering the distributions of conserved quantities in this system, higher moment analysis provide a scope to understand some existing problems. In this work we are looking at the higher moments of such multiplicity distributions.

Chapter 1

Introduction

How do these massive objects are formed? It was an all time interesting question, which is not yet completely answered. Always we were in a search for the building blocks of anything and everything. Thought about the fundamental particles, from which all matter has been built up, started for more that two thousand years ago. Then a field of science emerged which deals about this kind of questions and trying to answer something very fundamental in nature, that is the study of particles, the particle physics, began with the development of atomic theory, followed by a much deeper understanding about the quantized atom, then leading to the theory of the Standard Model and beyond. Through various experiments and theoretical models, now we have a set of particles, and again classifying them will turn out to remain on some elementary particles. The basic picture about particle physics will not be completed until we know how these particles are interacting. There are four fundamental forces through which particles in this universe interacts, *strong force, weak force, electromagnetic force* and *gravitational force*. This force is mediated by gauge bosons. The complete picture of elementary particles include particles from lepton family, quark family and these force carriers (figure 1.1). Each particle interacts with others differently, and these interactions can be well understood from the field through which they are interacting and the force carriers. There are different sub fields emerged which specifically explains each type of interaction. Quantum electrodynamics deals about the electromagnetic interactions while theory of weak interactions gives better understanding on weak interactions. Gravitation is widely studied and large experiments were designed to detect signature for this very weak force among the four. The field theoretical approach to understand strong interactions is quantum chromo dynamics [Oer06].

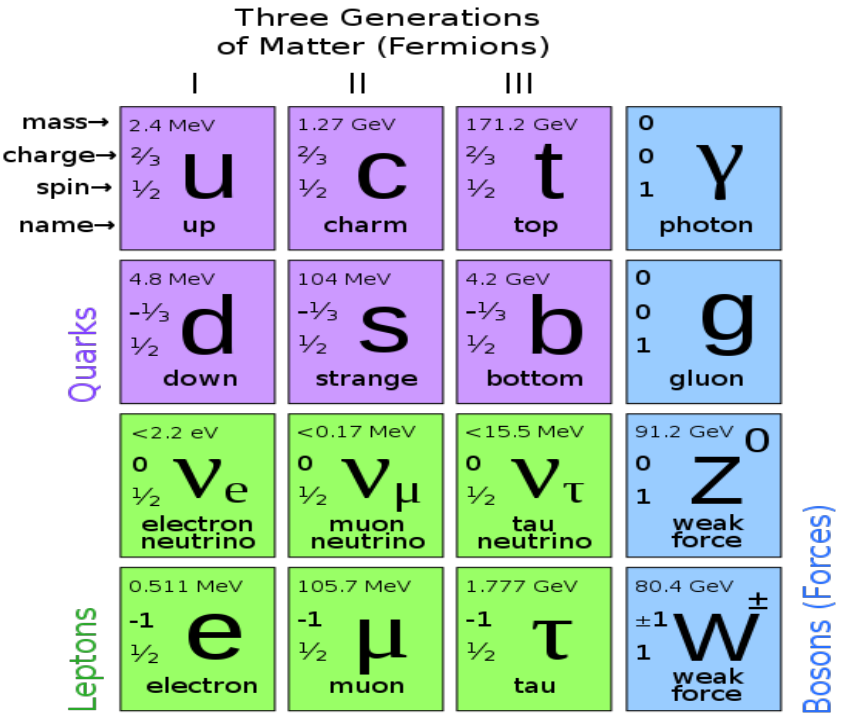

Figure 1.1: Diagrammatic representation of all elementary particles

1.1 Quantum Chromo Dynamics (QCD)

Quantum Chromo Dynamics is the field theoretical approach for describing the strong interaction.The particle content of this scheme can be broadly divided into two, quarks and gluons. Quarks are the set of fundamental particles which are the building blocks of mesons and hadrons, where gluons are the strong force carriers in the system of quarks.

Three major concepts defines QCD and they are (i) coloured quarks, (ii) interaction between coloured quarks results from exchange of spin one, coloured gluon fields and (iii) local gauge symmetry. Briefly,

(i) Quarks comes under the fundamental constituents of matter with various intrinsic properties, including colour charge, electric charge,spin, and mass. There are six flavors of quarks which are detected from various experiments, up (u), down (d), charm (c), strange (s), top (t) and bottom (b). Quarks can come in three colours (e.g. red, green and blue). Another interesting property of quarks is that they posses fractional charges. But fractional charges, or simply, a single quark can not be observed in isolation. It is an experimental fact, and this result was explained by including a

new concept in the theory, which is the *colour confinement.* Due to colour confinement, we can not observe single quarks. Physically observable particles were formed by combination of quarks, but these combinations are colour neutral,examples are mesons, pions, kaons, protons and so on [O$^+$14].

(ii) The mass less, spin one bosons are the mediators of strong force, the gluons. It is analogous to the role of photons in QED. But the difference is, the photons are not self-interacting, while gluons are. There are eight types of gluons. This can be understood if one note that quarks (anti-quarks) can carry three colour charges. They can be combined in 9 different ways, one colourless state and eight coloured states. Gluons can not occur in a singlet state, because the singlet state can not interact with coloured states. Hence there are eight types of gluons mediating the strong force between quarks.

(iii) QCD is a gauge theory, i.e. Lagrangian is invariant under a continuous group of local transformations. SU(3) is the Gauge group corresponding to QCD. The QCD Lagrangian is,

$$L = -\frac{1}{4}F_a^{\mu\nu}F_{\mu\nu}^a + \sum_{flavors}\left[i\bar{\psi}\gamma^{mu}\left(\partial_\mu - ig\frac{\lambda_a}{2}A_\mu^a\right)\psi - m\psi\bar{\psi}\right] \tag{1.1}$$

with,

$$F_{\mu\nu}^a = \partial_\mu A_\nu^a - \partial_\nu A_\mu^a + g f_{bc}^a A_\mu^b A_\nu^c \tag{1.2}$$

A_μ^a is the gluon gauge field of colour a (a = 1,2,...,8), m is the bare quark mass, ψ is the quark spinor, and f_{bc}^a is the structure constant of the gauge group[Cha14].

These are the most basic understanding about QCD. But in order to understand more about the phenomena happening inside this theory, there we need to go deep into this basic properties and their physics. As discussed earlier, quarks interacts with each other by their *colour* charge. Colour charge is not a scalar sum of individual charges, colour charge is like a quantum vector charge. Even the quarks are fractionally charged, we can not observe single quark in isolation, because of colour confinement. It is an important consequence of low energy dynamics of strong interactions.Strong force increases with the increase of distance.

$$V(r) \approx \frac{\alpha}{r} + \sigma r \tag{1.3}$$

The strength of strong interaction is determined by the running coupling constant (α_s) which is analogous to the fine structure constant in quantum electrodynamics. As a consequence of the renormalization procedure the value of α_s depends on the amount of exchanged four-momentum between the interacting partons.

$$\alpha_s(|Q^2|) = \frac{12\pi}{(11n - 2f)ln(Q^2/\Lambda^2)} \tag{1.4}$$

where $|Q^2|$ is the square of the exchanged four-momentum (energy scale), n the number of colours in QCD (equal to 3), f the number of quark flavours (equal to 6) and $\Lambda_{QCD} \sim 300MeV/c$ is a constant calculated from experimental data.[Cha14] A key property of QCD is that $11n - 2f > 0$. As a consequence, α_s decreases with increasing energy scale (decreasing distance). This is called *asymptotic freedom*. When the energy of the system increases, the coupling between the particles will reduce. As a result the particles will be free to move over larger volume. This predicts a *phase transition*, from hadronic to partonic matter[ABMRS17]. Experimentally also, this predictions valid. That means, if we collide heavy nuclei with high energy, and thus creating same kind of a critical condition, like an asymptotically free partonic matter. There are several attempts to understand about this particular phase transition which is governed by quantum chromodynamics [BBC$^+$90]. Both theoretical and experimental studies trying to get the phase diagram for this particular transition. Lattice gauge theory is a theoretical approach while heavy ion collisions are experimental approaches. But before that one needs to understand about the new phase of matter.

1.2 Quark Gluon Plasma (QGP)

Let us begin with a very simple picture. We know nucleons are incompressible, and closely packed by quarks, and it would contribute the high density limit of matter. Also we know that, nucleons are really composite, bound states of point like quarks. Then, if we increase the density some how, they will start to overlap. It will continue until we reach a state in which each quark are no longer bound, and finds a considerable number of other quarks within its immediate vicinity. There is no way to identify which of these had been its partners in a specific nucleon at some previous state of lower density. So after a certain point, the concept of a hadron thus loses its meaning, and the system transformed from nuclear matter to a system whose basic constituents are unbound quarks. They can move freely over

a nuclear volume rather than a nucleonic volume and the state of matter at that stage can be described in terms of fundamental constituents like quarks and gluons. This deconfined state of matter is commonly known as $QuarkGluonPlasma$ (QGP)[Cha14][Sat11].It is a nearly thermalised state of matter.

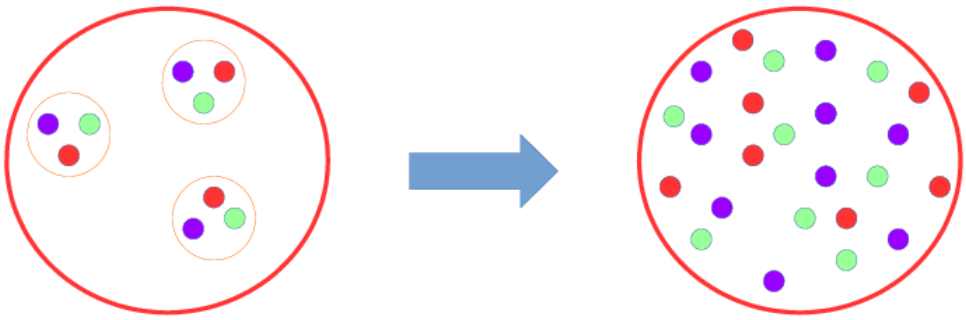

Figure 1.2: Hadrons to QGP transition[Sal09]

The mechanism of deconfinement can be explained by the screening of the colour charge. It is analogous to the Mott transition[Cha14]. In dense matter, the long range coulomb potential plays a role to bind ions and electrons into electrically neutral atom. It is partially screened due to presence of other charges. Then the Coulomb potential become much more short range,

$$V(r) = e_0^2/r \rightarrow e_0^2/r \times exp(-r/r_D) \tag{1.5}$$

here r is the distance from the probe to the test charge. r_D is the Debye screening radius and is inversely proportional to density,

$$r_D \sim n^{-1/3} \tag{1.6}$$

At enough high density, r_D can be smaller than the atomic radius. Then a given electron can no longer feel the binding force of its ion, alternatively, at such density the Coulomb potential can no longer bind electron and ion into a neutral atom. The previously insulating matter becomes a conducting matter then. This is the Mott transition in atomic physics[Cha14]. We expect deconfinement to be the quantum chromodynamic analogue of Mott transition. The quarks can not be bound into a hadron, due to the screening of colour potential. The wondering fact in this analogy is the very different nature of QCD and QED forces. Interaction potential in QED is,

$$QED : V(r) \sim -e^2/r \tag{1.7}$$

Comparing QED and QCD potential,in QED, potential decreases continuously with increasing distance, while in QCD, it increases with distance. However, screening is a phenomenon dominating at high density,which occurs at short distance. The difference in QED and QCD at large distance does not have any consequence then. In QCD, interaction strength decreases at short distances because of asymptotic freedom, thereby enhancing the deconfinement.

1.2.1 Importance to study about QGP

There are several models, which tells about the origin of universe. Among those the most prominent and well accepted theory is the *Big-Bang Theory*. According to this theory, QGP was the first state of matter during the expansion of universe[Cha14].

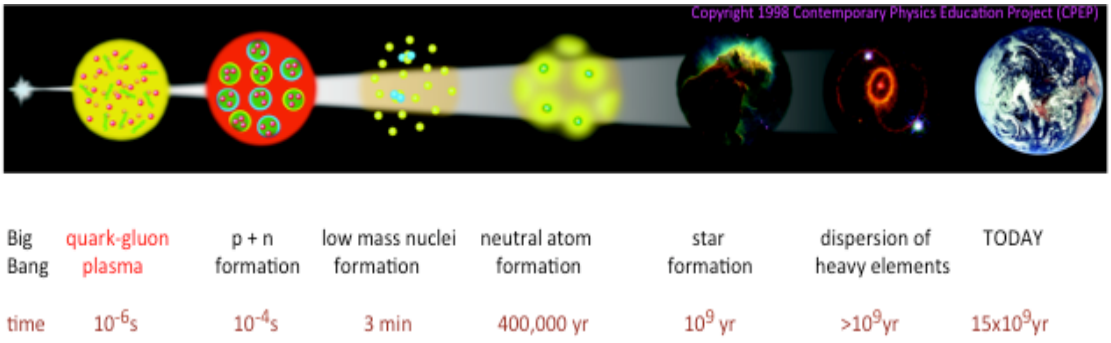

Figure 1.3: Diagrammatic representation of Big-Bang, various stages and their time evolution

At the earliest time of universal expansion, temperatures are of the order of $T \sim 10^{19}\,GeV$, it is the Plank scale temperature. We do not have much understanding on this time, but we have better understanding of the later stage of evolution,around temperature $T \sim 10^{16} GeV$. It is the Grand unification scale. In Grand unification scale, strong and electroweak interactions are unified. The universe at this scale may also be super symmetric. As the universe further expands and because of that it cools. Then the strong and electroweak interactions are separated. At much lower temperature $T \sim 100\,GeV$, electroweak symmetry breaking takes place. Baryon asymmetry may be produced here[Cha14]. Universe existed as QGP, which is the deconfined state of quarks and gluons, that was the first state of matter. Deconfinement-confinement transition occurred somewhere around $T \sim 100\,MeV$, and hadrons were formed. Relativistic Heavy Ion collider (RHIC) at Brookhaven National Lab-

oratory (BNL), and Large Hadron Collider (LHC) at European Organization for Nuclear Research (CERN), are designed to study matter around this temperature. At temperature $T \sim 1\,MeV$, nucleosynthesis starts and light elements were formed. This temperature range is well studied in nuclear physics experiments. At temperature $T \sim 1\,eV$, universe changes from ionized gas to a gas of neutral atoms and structures began to form. There are predictions about the existence of QGP in celestial objects, such as at the core of a neutron star. Neutron stars are remnants of gravitational collapse of massive stars. They are small objects with radius $\sim 10\,Km$, but very dense compared to normal nuclear matter. At such high density hadrons will loss their identity and matter is likely to be in the form of QGP. One important difference between QGP at the early universe and that in neutron stars is the temperature. While in early universe, QGP was at temperature $T \sim 100\,MeV$ but at the core of the neutron star it is cold QGP, temperature is about $T \sim 0\,MeV$. Other signature of QGP can be found in supernova explosions, where hot and dense matter with energy density exceeding $1\,GeV/fm^3$[Cha14]. Collisions between neutron stars or between black holes can also create such a condition.

1.3 Higher moments and QCD

Probability and statistical theory comes into picture when we have to deal with a number of events, and to study about their properties. Since it is a collection of events, it will follow a distribution, with some parameters. This parameters are the defining quantities of that distribution and the number of parameters change from one distribution to other. The main two parameters widely used are the mean (μ) and the standard deviation (σ). The mean of a distribution gives the average value or the expected value of events, while standard deviation indicates the variation of each events in that distribution from its mean value. But the distribution we are getting from our day to day life may not be a perfect one. That means, it can have deviations or asymmetries from the actual defined distributions of that kind. So we need to have some measure on those asymmetries, which are done by moment calculation. Mathematically, mean is the first moment, whereas σ is the square root of second moment of the distribution. As we go to higher moments, which are more sensitive towards the nature of distribution, we will get a good measure on the asymmetry and through that a good understanding about the system under research.

These higher moments play a very important role in heavy ion collisions also. Many approaches taken to understand the heavy ion collisions are based on statistical analysis. So there the study of higher moments are successful in describing those system. Details about higher moment study in heavy ion collisions and its relation with QCD is very important to understand in this case[Taw13].

1.3.1 Mathematical framework of higher moments

Moments can be calculated from the probability density function. For all real valued random number x, we can define a probability density function $f(x)$. Then the raw moment is,

$$m_n^{'} = \int_{-\infty}^{+\infty} x^n f(x) dx \Rightarrow m_n^{'} = \langle x^n \rangle \tag{1.8}$$

There is another alternative to moments, that is cumulants. The relation which connects moments and cumulants can be written from a recursion formula as given below,

$$C_n = m_n^{'} - \sum_{m=1}^{n-1} \binom{m-1}{n-1} C_m m_{n-m}^{'} \tag{1.9}$$

From this equation, the following is just a few examples of relation between moments and cummulants up to fourth order.

$$c_1 = m_1 \tag{1.10}$$

$$c_2 = m_2 \tag{1.11}$$

$$c_3 = m_3 \tag{1.12}$$

$$c_4 = m_4 - 3m_2^2 \tag{1.13}$$

These are the raw moments and cumulants. There is another quantity of interest is the central moment. Central moments are calculated with respect to the mean value, where raw moments are calculated with respect to zero. The n^{th} order central moment can be written as,

$$m_n = \int_{-\infty}^{+\infty} (x-\mu)^n f(x) dx \Rightarrow m_n = \langle (x-\mu)^n \rangle \tag{1.14}$$

The common feature of these two kind of moments are, their zeroth order moment is always one. In the case of central moment, the first order moment will be zero. The second central moment is variance. Another interesting parameter is the $skewness\,(S)$. The value of skewness represent the asymmetry of the distribution in a particular direction. For example,

a positively skewed distribution will have a longer tail in the right side and for negative value of skewness will show a longer tail in left side. One more parameter we are using in this work, $Kurtosis\,(\kappa)$. it is used to quantify the peakedness of the distribution. Collectively, the following relations are the defining structures of mean, variance, skewness and kurtosis with the cumulants.

$$M = c_1 \tag{1.15}$$

$$\sigma = \sqrt{c_2} \tag{1.16}$$

$$S = \frac{c_3}{(c_2)^{3/2}} \tag{1.17}$$

$$\kappa = \frac{c_4}{(c_2)^2} \tag{1.18}$$

Some ratios of these parameters are also very useful for statistical analysis, which are given below,

$$\kappa\sigma^2 = \frac{c_4}{c_2} \tag{1.19}$$

$$\frac{\sigma^2}{M} = \frac{c_2}{c_1} \tag{1.20}$$

$$\frac{\kappa\sigma}{S} = \frac{c_4}{c_3} \tag{1.21}$$

1.3.2 Connection of higher moments with QCD

We are approaching the problem in a statistical way, where we are considering the system as an ensemble with some macroscopic parameters like $pressure\,(P)$, $temperature\,(T)$, $chemical\,potential\,(\mu)$, $volume\,(V)$ and $number\,of\,particles\,(N)$ [M07]. This number of particles will also follow some distribution, and analyzing the properties of that distribution can lead us to the information about the existence of QGP and its properties. There are three types of ensembles, in order to describe the system which we are studying [M07]: canonical, micro canonical and grand canonical ensemble. In canonical ensemble the system can exchange energy with the surroundings, but not the particles. But in micro canonical ensemble, the energy and number of particles in the system is fixed, no exchanges are allowed. In the case of grand canonical ensemble, the system and surrounding can exchange both the energy and the particle[Taw13]. There are three conserved quantities in QCD, $baryon\,number\,(B)$, $strangeness\,(s)$, and the $charge\,(Q)$. Conserved quantities will give us an opportunity to study about the system in a different way. Their fluctuations over system can give important results on the parameters which we are looking for. The

susceptibility of the system plays an important role here. Susceptibility, χ, of a system tells us the response of that system to some perturbation. The generalized susceptibility of conserved quantities are obtained by taking the derivative of dimensionless pressure as,

$$\chi^{BSQ}_{lmn} = \frac{\partial^{l+m+n}\left(\frac{P}{T^4}\right)}{\partial\left(\frac{\mu_B}{T}\right)^l \partial\left(\frac{\mu_S}{T}\right)^m \partial\left(\frac{\mu_Q}{T}\right)^n} \tag{1.22}$$

where B, S, Q are the conserved quantities of QCD, and l, m, n denotes the higher order derivatives. This susceptibility is also related to the moments of the distribution. For large number of events higher order moments can be calculated and it will give a good understanding about the QCD observables. Here are the the relation between susceptibility and higher moments (up to fourth moment),

$$mean : M = \langle N \rangle = VT^3\chi_1 \tag{1.23}$$

$$variance : \sigma = \left\langle (\delta N)^2 \right\rangle = VT^3\chi_2 \tag{1.24}$$

$$skewness : S = \frac{\langle (\delta N)^3 \rangle}{\sigma^3} = \frac{VT^3\chi_3}{(VT^3\chi_2)^{3/2}} \tag{1.25}$$

$$kurtosis : \kappa = \frac{\langle (\delta N)^4 \rangle}{\sigma^4} - 3 = \frac{VT^3\chi_4}{(VT^3\chi_2)^2} \tag{1.26}$$

From above equations, we can write a more generalized expression for the connection between the susceptibilities of conserved quantities and the cumulants,

$$c_n = VT^3\chi^n_q,\ q = B, s, Q. \tag{1.27}$$

In the experiment, we can measure the net-baryon number (ΔB), net-strangeness (Δs) and net-charge (ΔQ) on an event by event basis. This equation is a powerful expression, where the left hand side is the experimental observable and the right hand side is QCD observable. This is why the study of higher moments (cumulants) of conserved quantities is an excellent tool to understand about QCD observables, and from there to get information about QGP [Eji08]. There is another important assumption, which we are considering in the analysis of heavy ion experiment. From the experiment, we are able to see only a section or a slice of actual phase space. It is because of the technologies we have developed is not yet efficient to create and measure the actual situation. So when we are studying the physics in that slice, we are assuming that it will be similar in all other slices, in the case of conserved quantities. If the system formed during collision is uniform, then the all slices of total phase space should give equal result concerned about the conserved quantities.

1.4 A short review on Fluctuations in QGP

The higher moment calculation in this case will be more error prone, because the number which we are dealing is of the order of millions and more. So we did a review till second order moment. There we focused on the fluctuation study, because the fluctuation is an indication of the changes in the system, and it can give authentic explanations for the importance to have a higher moment study. We mainly done a number-ratio fluctuation [PGV02, CHS09].

The most straight forward way to check number-ratio fluctuations on an event-by-event [Hei01, SRS99] basis is by the ratio $\frac{N_a}{N_b}$. Because this moments of this quantities will not have any dependence with the unknown parameters like volume and temperature of the system. So this can be used as good measure for fluctuation analysis. The relative multiplicity can be defined as $\left(\frac{N_a}{\langle N_a\rangle} - \frac{N_b}{\langle N_b\rangle}\right)$. Variance of relative multiplicity can be written as,

$$\begin{aligned}
\nu_{(ab)} &= V\left(\frac{N_a}{\langle N_a\rangle} - \frac{N_b}{\langle N_b\rangle}\right) && (1.28)\\
&= \left\langle\left(\frac{N_a}{\langle N_a\rangle} - \frac{N_b}{\langle N_b\rangle}\right)^2\right\rangle - \left\langle\left(\frac{N_a}{\langle N_a\rangle} - \frac{N_b}{\langle N_b\rangle}\right)\right\rangle^2 \\
&= \frac{\langle N_a^2\rangle}{\langle N_a\rangle^2} - 2\frac{\langle N_a N_b\rangle}{\langle N_a\rangle\langle N_b\rangle} + \frac{\langle N_b^2\rangle}{\langle N_b\rangle^2} && (1.29)
\end{aligned}$$

the ν would also provide the statistical part of total fluctuations. The $\nu_{(stat)}$ can be written as,

$$\nu_{(stat)} = \frac{1}{\langle N_a\rangle} + \frac{1}{\langle N_b\rangle} \tag{1.30}$$

So the dynamical fluctuation is the difference of total fluctuation and the statistical fluctuation.

$$\begin{aligned}
\nu_{(ab,dyn)} &= \nu_{(ab)} - \nu_{(stat)} && (1.31)\\
&= \frac{\langle N_a^2\rangle}{\langle N_a\rangle^2} - 2\frac{\langle N_a N_b\rangle}{\langle N_a\rangle\langle N_b\rangle} + \frac{\langle N_b^2\rangle}{\langle N_b\rangle^2} - \frac{1}{\langle N_a\rangle} + \frac{1}{\langle N_b\rangle} && (1.32)\\
\nu_{(ab,dyn)} &= \frac{\langle N_a\left(N_a-1\right)\rangle}{\langle N_a\rangle^2} - 2\frac{\langle N_a N_b\rangle}{\langle N_a\rangle\langle N_b\rangle} + \frac{\langle N_b\left(N_b-1\right)\rangle}{\langle N_b\rangle^2} && (1.33)
\end{aligned}$$

The following figures are obtained from this fluctuation study, were the ratios have been taken for the major hadrons we are obtaining in the collision. It also used the results from all available, leading heavy ion experiments for this. From the figure 1.4, it is evident that there exist fluctuation. For low energy experiments it is less than zero, and for high energy

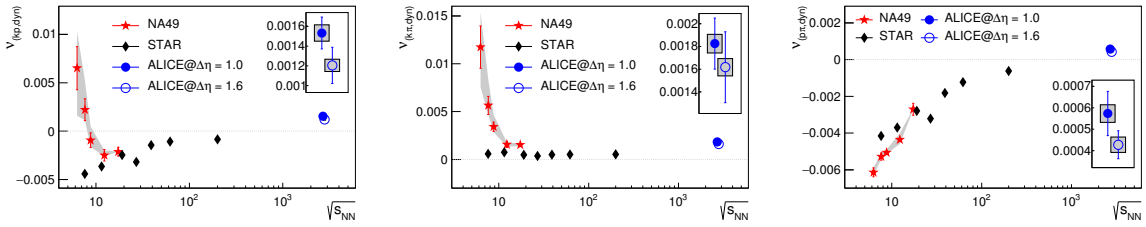

(a) (b) (c)

Figure 1.4: Dynamical fluctuation with particle ratios[Ars16] (a) kaon-proton ratio,(b) kaon-pion, (c) proton-pion

regime it is positive. The results from cross ratio not only shows the existence of fluctuation, but also gives an indication that each quantum numbers are correlated during the creation. A perfect cross over in the fluctuation graphs is another important feature. The plot is for dynamical fluctuation, and the cross over is an indication of change in the system which is not just non-equilibrium effects. This gives a scope for higher moment analysis in this energy level [A$^+$09, A$^+$15].

1.5 Experimental background

From the QCD predictions, it was clear that we can create a system which is deconfined, from the high energy and high density collisions of heavy nuclei. The experiments which are designed to check this predictions are the key to unrevealing the physics behind the QGP[Sal09]. The main motivation for this kind of experiment is that, in the collision at very high energy, the colliding nuclei will have a large energy compared to their rest mass. This energy is deposited over a small volume for a short interval of time. In this region the density of energy is so large that it may favour the appearance of new forms of matter. The search for these new forms of matter is the central objective of heavy-ion physics. We use heavy nuclei because they are rich in quark content compared to proton.

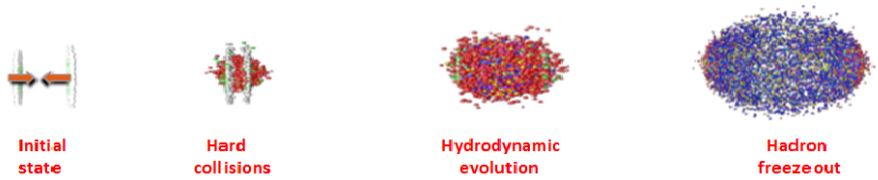

Figure 1.5: Schematic representation of heavy ion collision[Cha14]

The figure 1.5 shows the diagrammatic representation of what is happening exactly in the experiment. After collision of two heavy nuclei, those two nuclei will collapse and form a fireball. Since we are providing very high energy to this nuclei, that energy will be deposited in this fireball, which is very dense by the quark matter of nuclei. This fireball is expected to be in a deconfined state. But this state is very unstable, because we are depositing very dense and highly energetic particles in such a small volume. So the existence of this state will be very small. Because of the large internal pressure of the system itself, it will start to expand hydro dynamically[JHZ16]. As the system expands, it will start to cools down and that will result in the hadronization. Hadronization is the production of hadrons. These producing hadrons will be detected using specially designed detectors with respect to their momentum, energy, position and so on. Each particle produced in the event is know as a track and the total number of outcoming particles in an event is known as the multiplicity of that event[Sal09].

There are different ways to know whether the QGP is formed in this collisions or not. To disentangle the short existence of this new state, we need to have different probes. We can study about the two particle correlations, jet quenching, J/ψ production and looking into the properties of the hadrons produced. There are many approaches for this and different experiments were running at different energy scales all over the world. Here I am briefly discussing about the initiatives and experiments done and currently running in this area[Cha14][Sal09].

1.5.1 Heavy ion collisions

In 1970, Lawrence Berkley national Laboratory was built at Bevalac, where a transport line was built to bring heavy ions from Hilac (Heavy ion linear accelerator) to the Bevatron. That was the starting point of heavy ion collisions. The demonstration that excited nuclear matter could be studied gave birth to research programmes at Brookhaven National Laboratory (BNL) and at the European Organization for Nuclear Research (CERN)[Sal09]. Initially, BNL carried out experiment at a center of mass energy,$\sqrt{s} = 5\,GeV$ with gold (Au) atoms, and followed by CERN did its experiment with lead (Pb) atoms at $\sqrt{s} = 17\,GeV$. Those were fixed target experiments. Even though this energy was not sufficient to fully create QGP, it showed the existence of collective behaviour in heavy ion collisions. There were the signature of J/ψ suppression, which is an evidence for the colour screening. One

biggest mile stone in the heavy ion experiment is the discovery of QGP in RHIC at BNL in 2000. There are two detectors currently working in RHIC, STAR and PHENIX. The PHOBOS and BRAHMS were completed their operation [RHI]. STAR is designed to aim at the detection of hadrons while PHENIX is specialized in detecting rare and electromagnetic particles. PHOBOS has the largest pseudo rapidity coverage and it is dedicated for the bulk particle multiplicity measurements, while BRAHMS is designed for momentum spectroscopy [wik]. With the beginning of heavy ion experiments in CERN, another important mile stone was created. The ALICE experiment, at LHC, has been designed for this purpose. The energy at which LHC is working will be high enough to allow a careful investigation of the properties of this new state of matter, QGP. The temperature achieved will exceed by far from the critical value predicted for the transition to take place. The major pathways in the experiment starts from Linear Accelerator 3 (LINAC 3). It started up in 1994 and it is the starting point for the ions used in experiments at CERN [ALI]. It provides lead ions for the Large Hadron Collider (LHC) and for fixed-target experiments. Linac 3 will inject lead ions into the Low Energy Ion Ring (LEIR),which is used as a storage and cooler. It is providing ions to the Proton Synchrotron (PS) Booster with an energy of $72\,MeV/nucleon$. Ions will be further accelerated by the PS and the SPS (Super Proton Synchrotron) before they are injected into the LHC where they reach an energy of $2.76\,TeV/nucleon$.

1.6 Kinematics of Heavy ion collision

The outcoming particles from heavy ion collision, are having the knowledge about the system which is formed during the collision. So we have to study more about the properties of these particles in order to understand the QGP phase. The particles produced in heavy ion collisions are relativistic in nature. So we need to develop an analytical method to deal with those relativistically energetic particles and their properties. Hence we have to first understand the kinematics of heavy ion collisions, because we are trying to recreate a scenario in the early universe using experimental technology available to us. Here I am discussing a few key kinematic features used in heavy ion collisions.

1.6.1 Space Time picture

The figure 1.6 is about the collision of two nuclei in (t,z) plane. Two Lorentz contracted nuclei approaching each other with velocity of light and collide at (t=0,z=0). A fireball is created in the collision process. It expands in space- time and going through various processes till the created particles freeze-out.

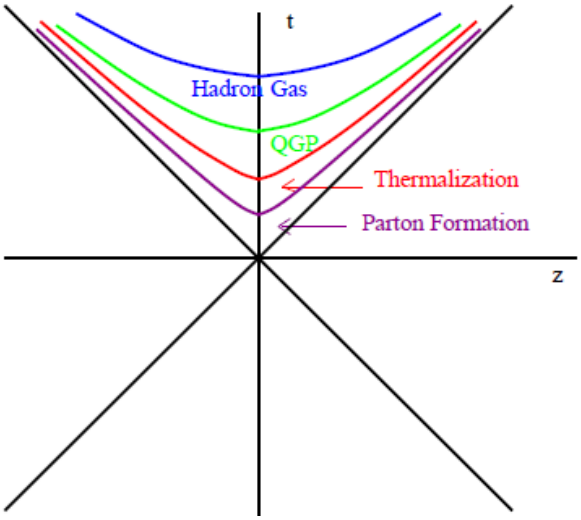

Figure 1.6: A space-time diagram for the evolution of matter produced in relativistic heavy ion collisions[Cha14]

In relativistic mechanics, we know Δt and Δx are not invariant distances, while the invariant quantity is $\Delta\tau^2 = \Delta t^2 - \Delta x^2$. So we can redefine the coordinates in relativistic collision,the proper time and space-time rapidity,

$$proper\,time : \tau = \sqrt{t^2 - z^2} \tag{1.34}$$

$$space - time\,rapidity : \eta_s = \frac{1}{2} ln \frac{t+z}{t-z} \tag{1.35}$$

1.6.2 Rapidity variable and Pseudo-rapidity variable

In relativistic mechanics,rapidity variable is defined as,

$$y = \frac{1}{2} ln \frac{E + p_z}{E - p_z} \tag{1.36}$$

$$= \frac{1}{2} ln \frac{1 + \frac{p_z}{E}}{1 - \frac{p_z}{E}} = tanh^{-1}(\frac{p_z}{E}) = tanh^{-1}(\beta_L) \tag{1.37}$$

is more appropriate than the longitudinal velocity ($\beta_L = \frac{p_z}{E}$). Rapidity has the advantage that they are additive under a longitudinal boost. That is better explained as, suppose that

a particle with rapidity y in a given inertial frame. It will have a rapidity $y + dy$ in another frame which moves relative to the first frame with rapidity dy in the $-z$ direction. One can see this from the addition formula of relativistic velocity β_1 and β_2 [Cha14]. When a particle is produced at an angle θ, we can redefine the rapidity variable in such way that it use the information of the angle at which the particle has been formed.

$$\begin{aligned} y &= \frac{1}{2} ln \frac{E + p_z}{E - p_z} \\ &= \frac{1}{2} ln \frac{\sqrt{m^2 + p^2} + pcos\theta}{\sqrt{m^2 + p^2} - pcos\theta} \end{aligned} \tag{1.38}$$

At very high energy, the mass can be neglected ($p >>> m$),

$$\begin{aligned} y &= \frac{1}{2} ln \frac{p + pcos\theta}{p - pcos\theta} \\ &= -lntan(\frac{\theta}{2}) \equiv \eta \end{aligned} \tag{1.39}$$

η is known as the pseudo-rapidity variable, and we need only θ to determine the pseudo-rapidity variable[Cha14]. It is very convenient variable for experimentalist, when the details of a particle such as its mass, momentum and so on are not know, but the angle at which it is produced is known.

1.6.3 Collision centrality

Since we are dealing with nucleus in the experiment, we need to consider their extended spatial orientation. One important parameter in this collision is the $impact\,parameter\,(b)$. It is the center to center perpendicular distance of two colliding nuclei. It can be zero to 2R, where R is the radius of an atom, or the candidate in the collision[Sal09].

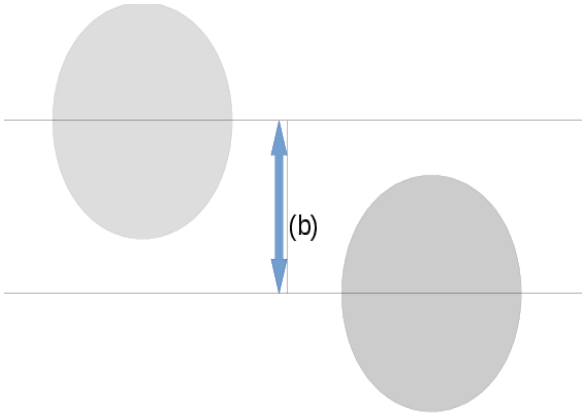

Figure 1.7: impact parameter (b)

Depending on the impact parameter, there are different types of collisions can happen. When two nuclei collide head on, it is a central collision, while a peripheral collision can occur when only glancing interaction occur between the two nuclei. The system created by these two types of collisions will be different qualitatively and quantitatively. So studying heavy ion collisions as a function of impact parameter can reveal different aspects of reaction dynamics.

We can not measure the impact parameter experimentally. But it is possible to have one to one correspondence between the observables like particle multiplicity, transverse energy and so on with the impact parameter. For example, one can assume that multiplicity or transverse energy is a monotonic function of the impact parameter. High multiplicity or high transverse energy events are from central collisions, and low multiplicity or low transverse energy events are from peripheral collisions[Cha14]. One can then group the collisions according to multiplicity or transverse energy.

Chapter 2

Statistical Analysis

2.1 Distributions and Models

In this work we are focusing on, how to deal with the multiplicity distribution of heavy ion collisions. From section 1.3.1, one can get the idea about, how the outcoming particle are important in the study of heavy ion physics. Since we do not have the information about the system formed during the collision, these multiplicity tracks are the pathway which carries the information about the system which we are interested[Taw13].

2.1.1 Binomial distribution

James Bernoulli (1654-1705) developed the understanding about binomial distribution. A binomial distribution or model is characterized by Bernoulli trials which either ends in success or failure. Suppose we have n trials and the probability of success on a trial is p [Ros07]. Then the conditions for which it is a binomial distribution:

- The Bernoulli trials are independent of each other.
- The probability for success, p, remains same for all trials.
- The number of trials n should be finite.
- The events should be discrete.

Definition

A random variable x is said to follow binomial distribution if it assumes non-negative values and its probability mass function is given by [Poi],

$$P(X = x) = \binom{n}{x} p^x (1-p)^{n-x} \tag{2.1}$$

Properties

- If probability for success and failure are equal, the given distribution will be symmetrical. If not, the distribution will be a skewed distribution.
- Mean of the distribution = E(x) = *np*.
- Variance = V(x) = *np(1-p)*.

2.1.2 Negative Binomial distribution

Negative binomial or Pascal distribution is a special case of binomial distribution. Let us consider a set of Bernoulli trials. It is used to describe the probability of $(r-1)$ successes and x failures in $(x+r-1)$ and $(x+r)$ trials respectively. The NBD probability density function is,

$$P_{r,p}(x) = \binom{x+r-1}{r-1} p^r (1-p)^x \tag{2.2}$$

In the case of multiplicity distribution in heavy ion collisions, negative binomial distribution is a good approximation at the lower center of mass energy regime. At lower energy scale, the multiplicity or the number of outcoming hadrons will be less. Even in binomial distribution, negative binomial distribution is the best match for multiplicity distributions[TW13].

2.1.3 Poisson distribution

Poisson distribution is also a discrete distribution were it counts the events over time. It is the named after Simeon Denis Poisson (1781-1840). This distribution differs from the binomial distribution in the sense that in binomial distribution, we count the number of success and number of failures, while in Poisson distribution, the average number of success in given unit of time or space is matters [Poi].

Definition

The probability that exactly x events will occur in a given time is as follows,

$$P(x) = \frac{e^{-\mu}\mu^x}{x!}, x = 0, 1, 2... \tag{2.3}$$

It is the probability mass function of Poisson distribution. Where μ is the average number of occurrences per unit of time.

Condition for Poisson distribution

Poisson distribution is the limiting case of binomial distribution under the following assumptions [Ros07].

- The number of trials n should be indefinitely large.
- The probability of success p for each trial is indefinitely small.
- $np = \mu$, should be finite where μ is constant.

Properties

- Poisson distribution is defined by single parameter μ.
- Mean = μ.
- Variance = μ. (Mean and Variance are equal)

At very high energy, the multiplicity also increases. Then Poisson distribution is a good approximation to the multiplicity distributions in heavy ion collisions[ABMRS17][BMFK$^+$12].

2.1.4 Skellam distribution

The distribution of the difference between two independent Poisson random variables was derived by Irwin (1937) for the case of equal parameters. Skellam (1946) and Prekopa (1952) discussed the case of unequal parameters. It is named as Skellam distribution.

Definition

It is the difference of two independent Poisson distributions with uncorrelated mean values. If μ_1 and μ_2 are the means of two different Poisson distributions, then the corresponding Skellam distribution's probability mass function is follows,

$$P(k;\mu_1,\mu_2) = e^{-(\mu_1+\mu_2)}(\frac{\mu_1}{\mu_2})^{k/2}\, I_k(2\sqrt{\mu_1\mu_2}) \tag{2.4}$$

where I_k is the modified Bessel function of first kind. From equation 1.27, we know how the higher moments of conserved quantities are related to QCD observable. Each particles produced in an event is best explained with Poisson distribution, at very high event rate. So

the conserved quantities which are basically the difference of this particles in a defined way, will give rise to a Skellam distribution[BMFK$^+$12]. From the particle content, pions can be termed as the proxy for charge, kaons for strangeness and protons for baryon number. So the study of higher moments of Skellam distribution is essentially serving as a probe for understanding the conserved quantities distribution across the event and their properties. The first four moments of Skellam distribution and some of the ratios derived from them are listed, in terms of the means of the Poisson distributions from which it is coming.

$$\mu = \mu_1 - \mu_2 \tag{2.5}$$

$$\sigma = \sqrt{\mu_1 + \mu_2} \tag{2.6}$$

$$S = \frac{\mu_1 - \mu_2}{(\mu_1 + \mu_2)^{3/2}} \tag{2.7}$$

$$\kappa = \frac{1}{(\mu_1 + \mu_2)} \tag{2.8}$$

$$S\sigma = \frac{\mu_1 - \mu_2}{\mu_1 + \mu_2} \tag{2.9}$$

$$\kappa\sigma^2 = 1 \tag{2.10}$$

2.1.5 Central Limit Theorem

Definition

Let $X_1, X_2, X_3...$ are the random variables from a distribution with a mean of μ and variance σ. Let $\bar{X}$ be the sample average of X_1, X_2..etc. Then the distribution of $\bar{X}$ will tend to be a normal distribution with mean μ and variance $\frac{\sigma}{\sqrt{n}}$ as the n tend to infinity [Ros07] [Poi].

Properties

- The distribution of $\bar{X}$ will tend to normal distribution as n is large. So the approximation improves as n get larger.
- The random numbers should be independent, and derived from a same distribution.

2.2 Monte Carlo Method

Since we are dealing with a probabilistic approach, Monte Carlo method is a good choice. Monte Carlo methods are a class of algorithms that functioning with randomness of events. Using randomness, this method is effectively trying to recreate and analyze some physical

system. In our experiment, the particles are coming in random fashion. Our objective is to study about them, in our labs. So simulation is the best option in such a scenario. Monte Carlo simulations are used because of this random nature. If we have probability distribution or a function, we can generate random numbers with respect to the given parameters. This way we can study about the multiplicity distributions, in way of recreating the events. In this work also we are using Monte Carlo simulations to generate events. Entire simulation and analysis are being done using object oriented software package ROOT.

2.2.1 ROOT: data analysis framework

ROOT is an object oriented data analysis frame work developed by physicists. It provides a very composite and fast platform for researchers to perform complicated and rigorous calculations. In high energy physics, one needs to satisfy many conditions to say an analysis tool is good. One important thing is to study about the experimental aspects, we need to create or manipulate data for such a model. Several parameters may need to check, several optimization conditions also. We can not try this things in actual experiment, because it is highly expensive and complicated. So the trial and error method we have perform in a model which is a miniature version of actual experiment. So the model validations and setting parameters which satisfy actual condition is quite a big task. Even if we are succeeded in that, how do we visualize the effects, the results of our various hypothesis. So the next important feature is the visualization of things. So we need to incorporate different visualization techniques, in this case graphs, plots, histograms, all these in all three dimensions. One needs to satisfy editing techniques also. That will help to modify the graphs and allows one to modify it i such a way that it is more efficient, accurate and perfect. We may need to save these outputs in a minimal space and use it for some further calculations. Another important feature is fitting data. The experimental outcomes are not well understood at the first glance. So we need to analyze it by different methods. One may needs to fit it with some predicted functions or may have to fit several functions to the given data. All these features are satisfied by ROOT. It has some well defined classes which enable the user to perform various analytical experiments with this. I will briefly explain some of the libraries or classes which are basic and used for my work.

- TF1 : It enable the user to define one dimensional functions in the program. Here the $integral$ function is available as predefined and we used that for our calculations.

- TFile : It is class dedicated for saving data to some file and reading data from a file.
- TH1F : This class is for plotting one dimensional histograms. We need to specify the number of bins needed and the range of x axis.
- TH2F : This one is also for plotting purpose, dedicated for two dimensional histograms. In a two dimensional histogram we need to specify number of bins in x and y axes. It is a good tool to save large number of one dimensional histograms in a compact form. It saves a lot of time while writing program and visualization is also good. We can get the projections along any axis and profile of the histogram in any direction, all these things are associated with this.
- TGraph : For the visualization of graphs we need to use this class. We can modify the plots in different colour, different point markers, different style, and also labeling and plotting multiple graphs in one chart is also included.
- TRandom : This class is very special for simulation studies. It is a powerful tool which helps the user to create random numbers which satisfy the user provided conditions. Different options are available even in this class, were $TRandom3$ is very good for best randomness. Because the computer generated random numbers are not exact random number, while they are pseudo random numbers.
- TCanvas : As the name indicates it gives a canvas for plotting all sorts of visualization methods. We can add multiple graphs in one canvas by dividing it into desired number of parts.

From these understandings, we can write a simple code in ROOT. Here comes the problem of which computational language is supported by ROOT, and the most favorable feature of ROOT is also that. It is basically built with a tolerance to C++ language but, one can write programs in C, $Python$, and R also [ROO].

Chapter 3

Data Analysis and Results

In order to calculate the higher moments, we need to create the multiplicity distribution from actual experimental data. The particles have been detected according to their transverse momentum, energy, position and so on. In this work we are focusing on the transverse momentum distributions of outcoming particles in the most central events. Then we are analyzing those data, extracted from experiments, to do Monte Carlo simulations using a data analysis frame work called ROOT. The higher moments are calculated for net charge, and validating CLT in this limit. All these computational work has been done for large number of events, in the High Performance Cluster(HPC), newly developed in our institute. The programs are really large, so we are showing only the part where the real calculations are being done. These part of codes are shown in Appendix-A.

3.1 Transverse momentum distribution

The figure 3.1 shows the transverse momentum distribution of particle yield. The y axis of the figure is a little complicated, but demonstrated in a very standard form. It is the rate of change of particles in a particular p_T bin collected in a defined rapidity window. Since we are assuming the fireball created is spherically symmetric, here we are dividing it by 2π, because of the azimuthal angle symmetry. Now we need to normalize the yield with respect to the total number of events happened, then only those data points will give an event- by-event scenario. Also, for further normalization with the momentum value, again it has to be divided by p_T [A$^+$02].

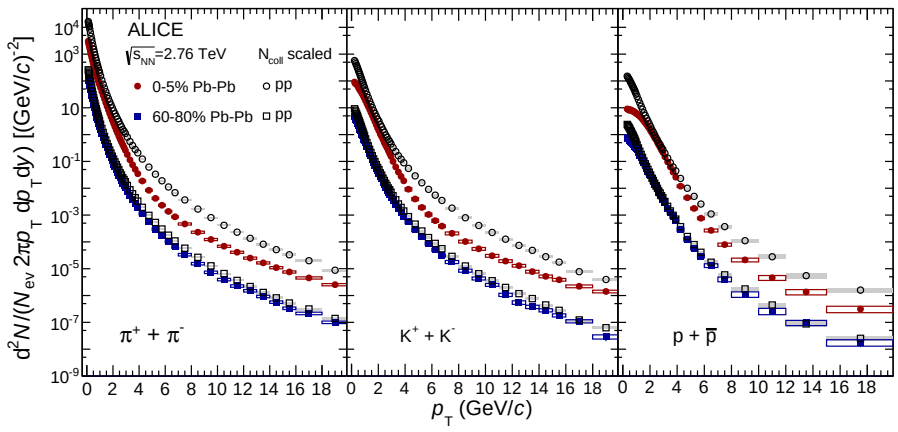

Figure 3.1: Transverse momentum distribution of hadrons[A$^+$14](pion,kaons,protons)

Integrating these graphs, and multiplying that value with $2\pi P_T$ will give the total number of particles produced in that transverse momentum range in the preferred rapidity window.

3.2 Approach and Results

From the transverse momentum distributions, data points were extracted in the ROOT format. This is the input for the program. Two different programs were developed in order to understand higher moments and to validate CLT. The data were available for pion, kaon, proton and anti proton. From there we chose a transverse momentum range which is available for all particles, and done the calculations. The sum of all positively charged particles (π^+, k^+, p^+) will give the total number of positively charged particles in the selected p_T window. Total number of negatively charged particles can be calculated in a similar way. Here we are dealing with four different particle id's, charged, pions, kaons, proton and anti proton as together, with two different charges, positive and negative [A$^+$13].

3.2.1 Producing higher moments

For the higher moment calculations, we have to construct the multiplicity distribution. The entire data set has been divided into ten p_T windows. These different p_T windows will enable us to understand the behaviour in bin wise and accumulated p_T range. Using predefined integral tools in ROOT, the p_T spectrum in each window has been integrated. This integration will give the number of particle produced in that p_T window. From the assumption that, the particles will follow Poisson distribution, our next goal was to create the

multiplicity distributions for those average number of particles obtained from the integration. Using Monte Carlo simulation, large number of events were generated and filled into a two dimensional histogram. The projection of that histogram along y direction will be a Poisson distribution with a mean of given value, which means it will be a multiplicity distribution with average number of particles produced in that p_T bin. Once we have the similar integral values for positive and negative particles of similar kind, their difference will give the net charge (Q) and sum will give total number of particles in that window. We have an insight about the distribution of charge, which will be a Skellam distribution. This procedure has been followed for all particle identities, and the projections about y axis have been plotted together, which is provided below,

Pions

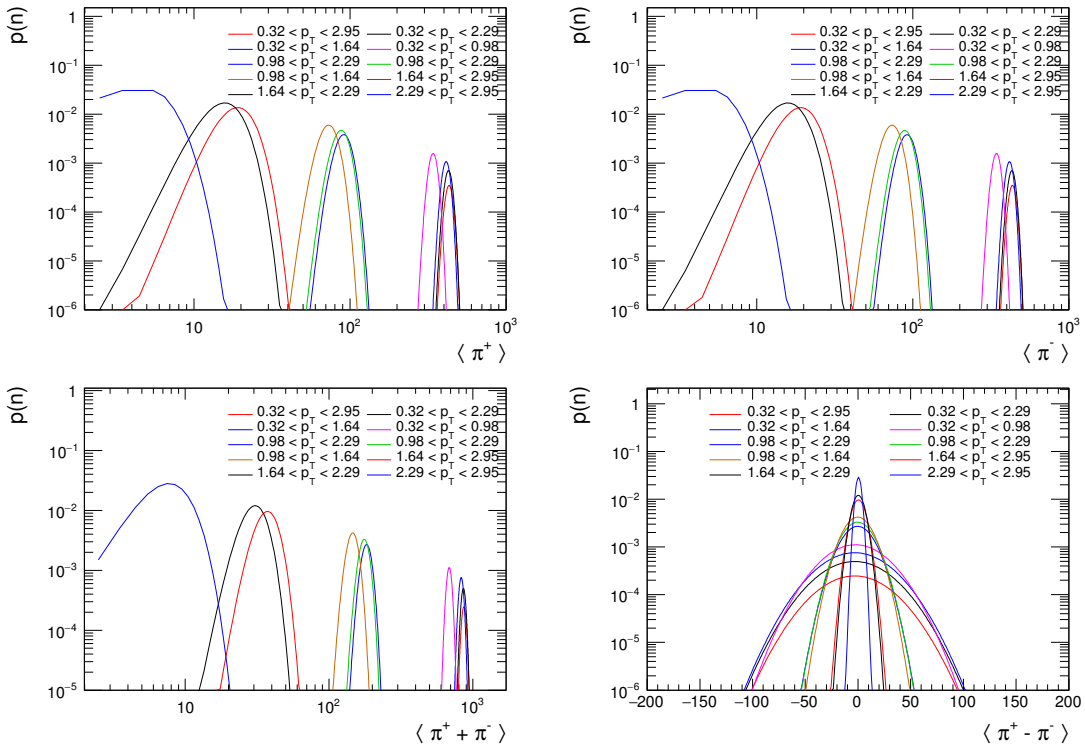

Figure 3.2: Top left panel shows the multiplicity distribution for positively charged pions whereas top right panel shows the multiplicity distribution of negatively charged pions. Bottom left panel shows the distribution of total pions ($< \pi^+ + \pi^- >$) and bottom right panel shows the distribution for net-particles ($< \pi^+ - \pi^- >$) estimated from the same events.

The above four plots (figure 3.2) are obtained from pion data. Pions are the hadrons which comprise around 80% of the total multiplicity. From the above plots, the top two are for

positively charged pions and negatively charged pions respectively. Their trend is as we were expected. Because, from the transverse momentum distribution, it is obvious that the number of particles detected will be less as we go to higher momentum range. The axis is in log scale, so the smaller plots have larger value. Bottom left figure corresponds to the sum of pion plus and minus particles. It should also looks similar to the independent distributions, just scaled up. The bottom right figure is the Skellam distribution for net-charge from pions. As we decrease the momentum bin, the spread has been decreasing and peaked distributions are obtained.

Kaons

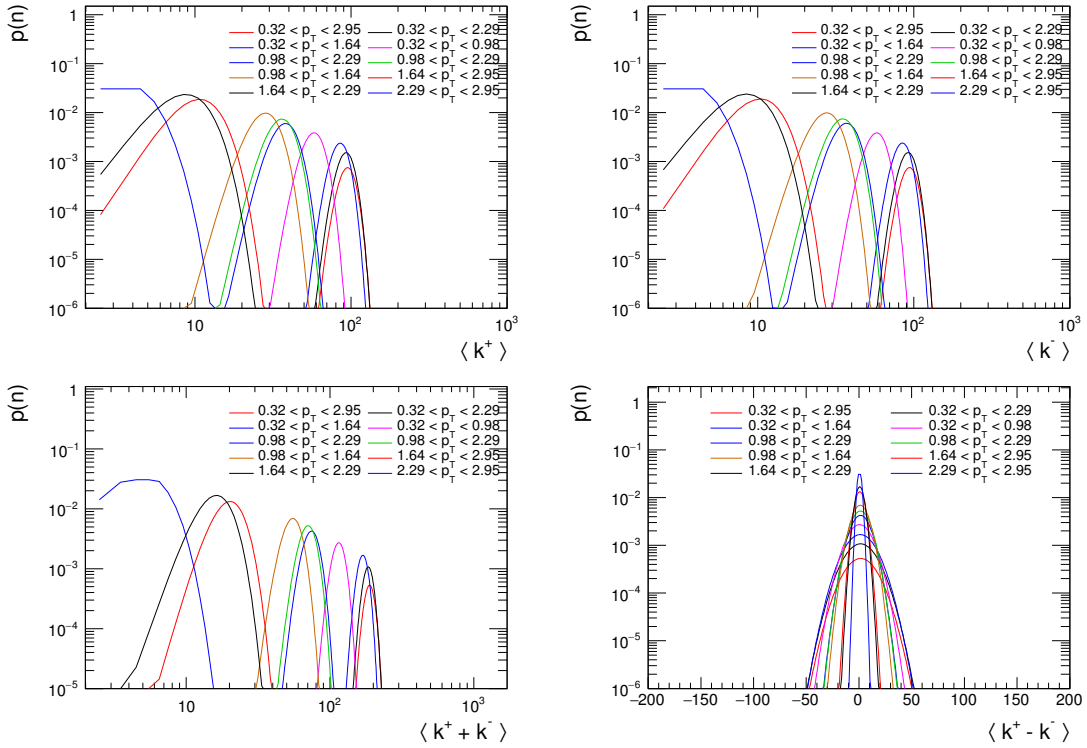

Figure 3.3: Top left panel shows the multiplicity distribution for positively charged kaons whereas top right panel shows the multiplicity distribution of negatively charged kaons. Bottom left panel shows the distribution of total kaons ($< k^+ + k^- >$) and bottom right panel shows the distribution for net-particles ($< k^+ - k^- >$) estimated from the same events.

In the total multiplicity, kaons contribute around 17%. For kaons also the distribution trend of positive and negative charged particles will look similar in the trend, and the sum of those will also follow same kind of a trend. The plots we are getting also matching with this. And here also, the net-charge distribution (bottom right figure) is showing a small spread as we

go to smaller bin size. But the entire distribution is less spread compared to the net-charge distributions for pions.

Protons

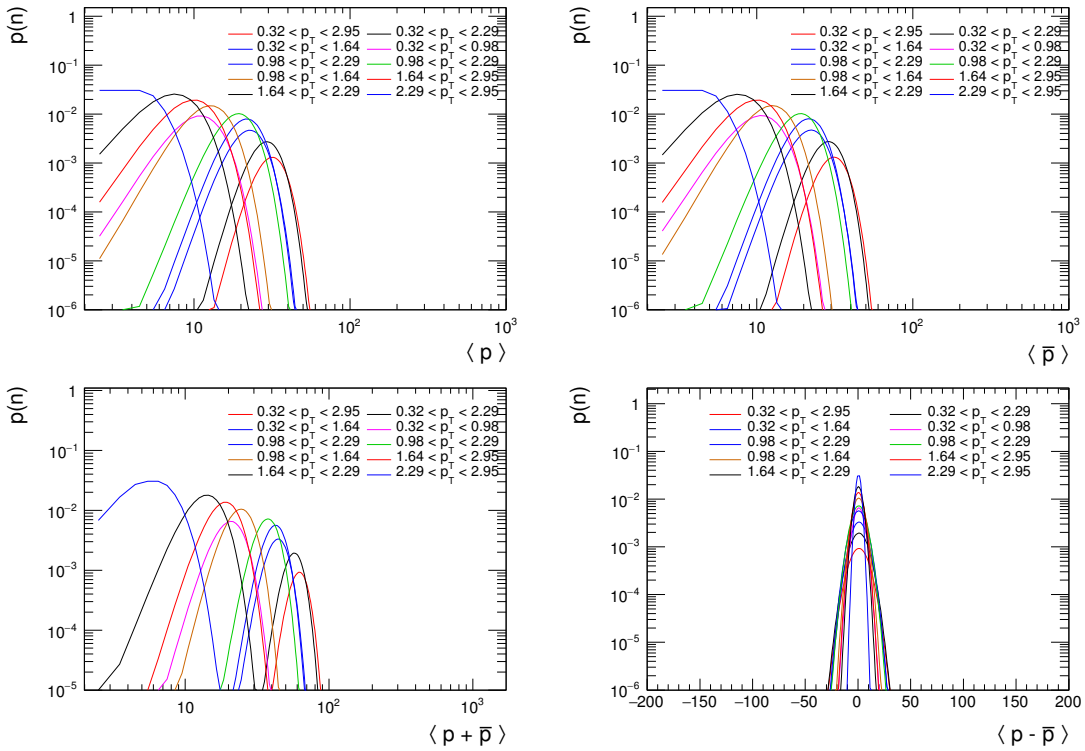

Figure 3.4: Top left panel shows the multiplicity distribution for protons whereas top right panel shows the multiplicity distribution of anti protons. Bottom left panel shows the distribution of ($< p^+ + \bar{p} >$) and bottom right panel shows the distribution for net-particles ($< p^+ - \bar{p} >$) estimated from the same events.

In the case of proton and anti proton, these are very small percentage of total multiplicity ($\sim 2\%$). There has to be a decrease in the spread of the multiplicity distribution, which is evident from the above figure, top two plots. Net-charge distribution became more narrower, which pronounce correlation with respect to the particle abundance in the system.

Charged particles

Charged particle distribution is an enclosure of all three particle identities we discussed earlier. So the expected trend for positive particles, negative particles and sum of particles are satisfying. One can easily understand the correlation from other individual particle distribution to this figures. The net-charge distribution is also matching with other same kind of distributions. Here we need to calculate the higher moments, to understand about

the spread and to get an idea about why it is like that.

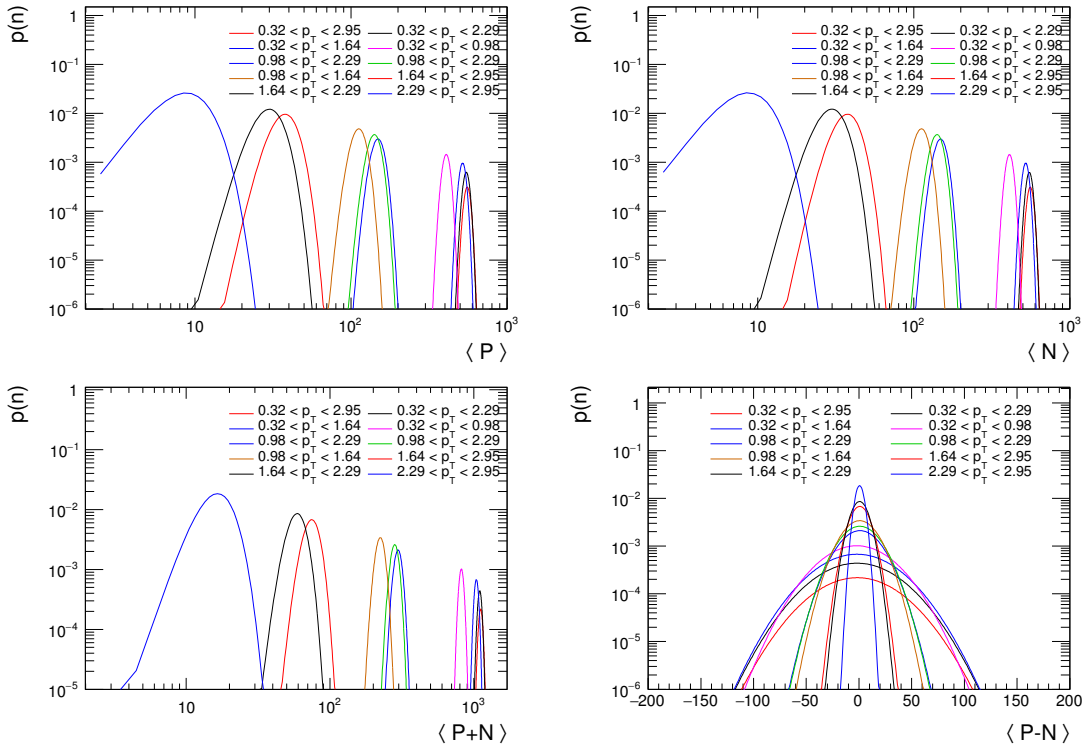

Figure 3.5: Top left panel shows the multiplicity distribution for positively charged particles whereas top right panel shows the multiplicity distribution of negatively charged particles. Bottom left panel shows the Distribution for total particles and bottom right panel shows the distribution for net-particles ($< P - N >$) estimated from the same events.

Once we have the distributions for the interested quantities in the system, next step is to calculate higher moments. In order to get higher moments from ROOT, we can use predefined statistical tools. First four moments (M, σ, S, κ) were calculated and plotted together for all four particle identities as defined initially in this section. The first plot is labeled with particle id's, for which colour code has been used, it is similar for all other plots. By analyzing figure 3.6 and figure 3.7, mean and σ for the positive and negative particles shows a decreasing behaviour with the decrease of momentum binsize. There is not much difference in the higher moments of these two sets. These two moments are higher for large sized particle identity, that is total charged particles, and small for protons. But the other two moments showing a different trend, were the order is just reversed. This behaviour can be understood from equations 1.17 and 1.18. The skewness and kurtosis is inversely related to second moment. So those will be large for the set of data which is having smaller second

moment. That is why we are getting the trend as like this. The figure 3.8 is for the sum of particles, which is also behaving like the individual distributions.

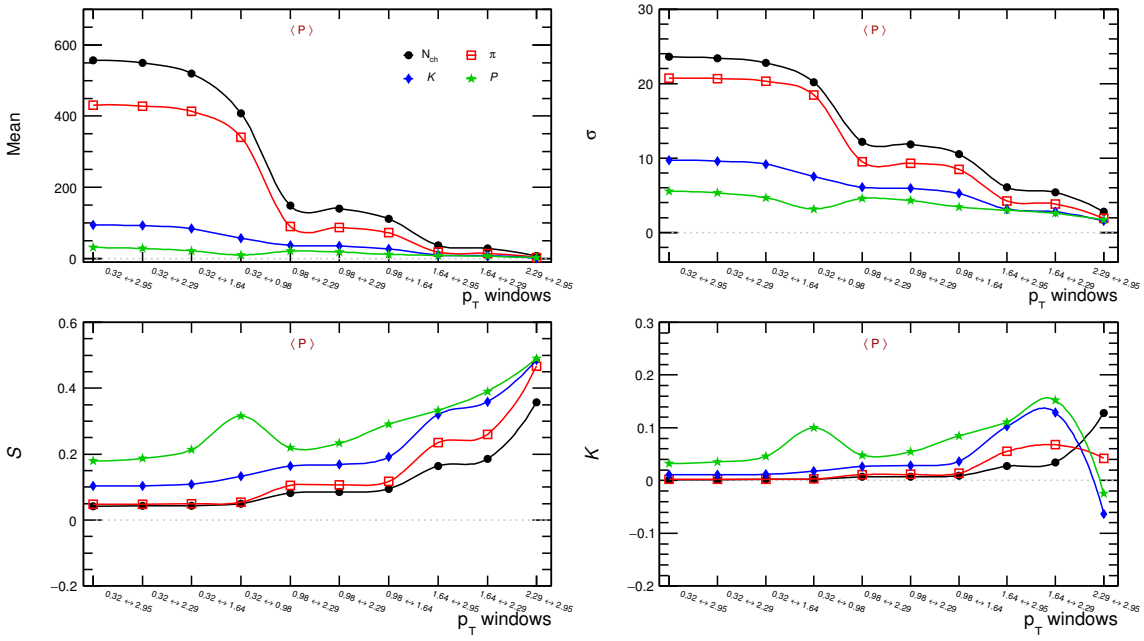

Figure 3.6: Higher moment plots for positively charged particles (π^+, k^+, p^+, and positively charged total particles).

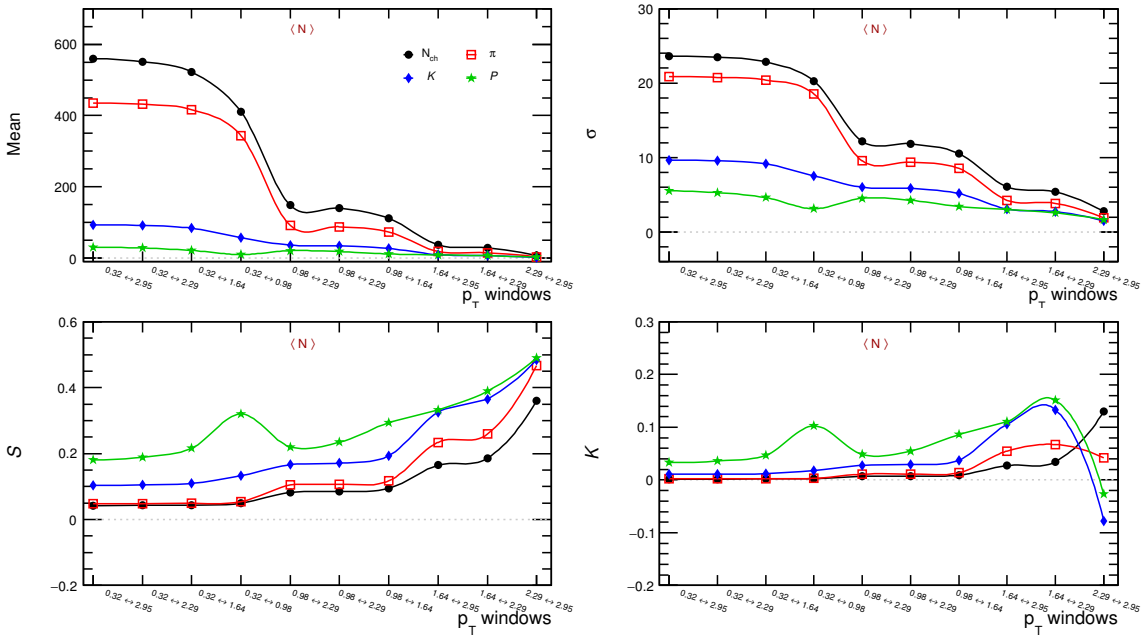

Figure 3.7: Higher moment plots for negatively charged particles (π^-, k^-, $\bar{p}$, and negatively charged total particles).

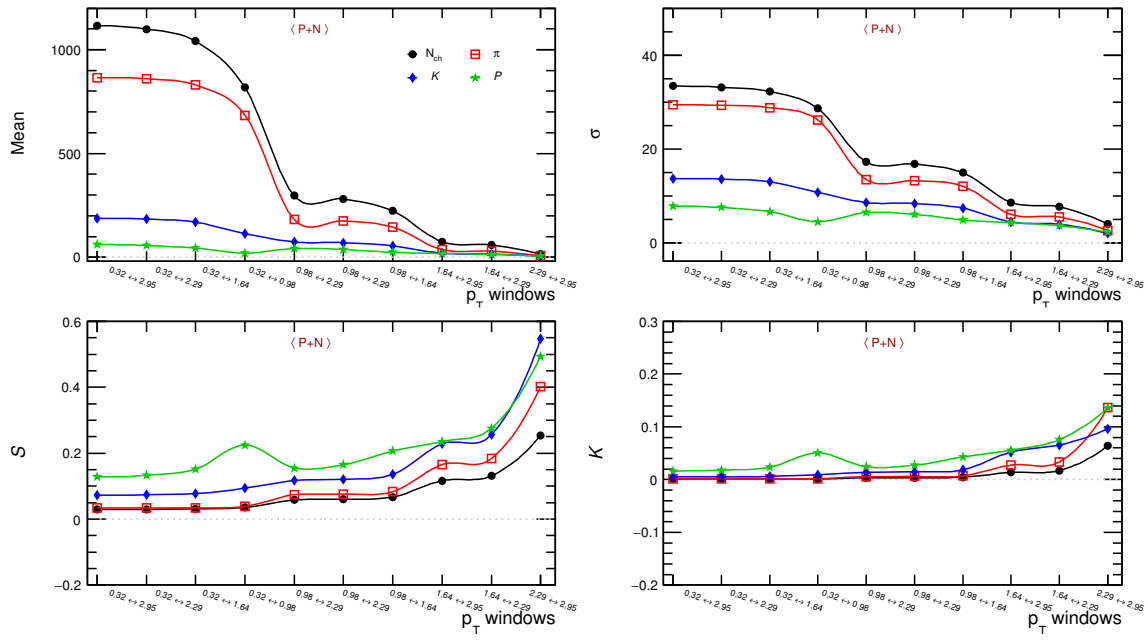

Figure 3.8: Higher moments for total particles in the event

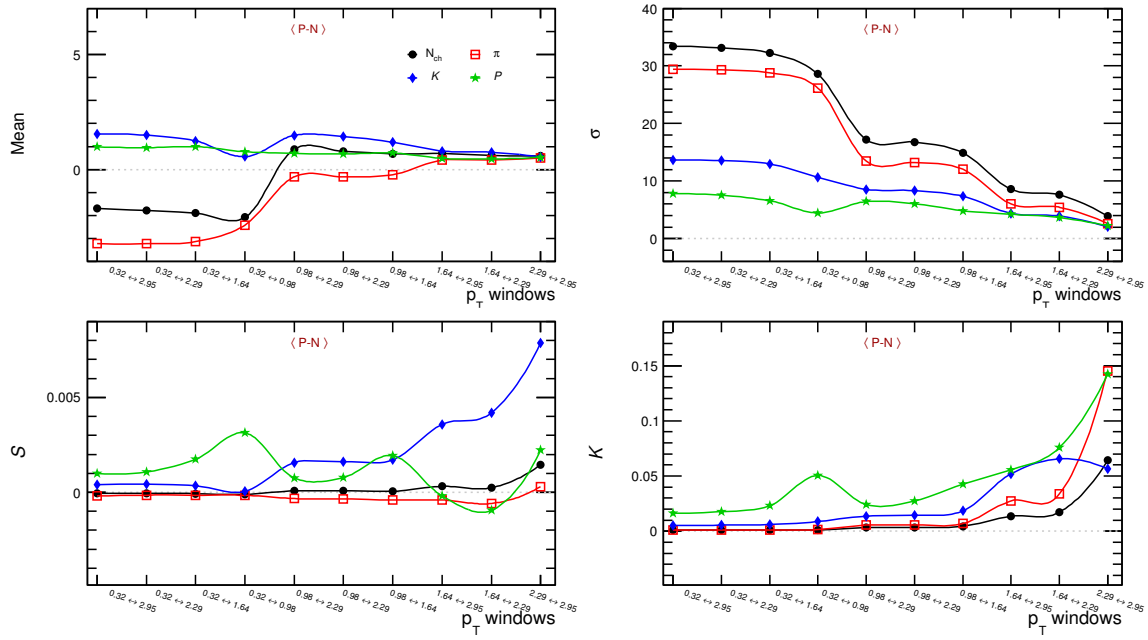

Figure 3.9: Higher moments for net-charge.

In figure 3.9, mean is almost stable for protons, slight changes in kaon system, but its very fluctuating for charged particles and pions. The second moment is again showing a decreasing trend with respect to the number of particles in each set. The spread is very large in charged particles while it is small in proton and anti proton distributions. Skewness is almost similar for all particles except for kaons. In the case of kaons and protons, there are

several anomalies in there production and behaviour. These hadrons are produced directly from the system, but it is coming from the decay of certain other particles. The problem is that, the direct production will have a non-biased number of both positive and negative particles, but the production through decay will be biased. It will cause the changes in the distribution and properties of these hadrons, which are not yet understood properly. The kurtosis is also showing such a change.

3.2.2 Higher Moments for Other relations

The above quantities are used to calculate the traditional higher moments as the net-particles are conserved in QCD. We propose some other quantities which are the ratios as well as two-particle correlators of all those particles which represents the conserved quantities of QCD. Namely, (1) $\left\langle \frac{P}{N} \right\rangle$, (2) $\left\langle \frac{N}{P} \right\rangle$, (3) $\left\langle \frac{P-N}{P+N} \right\rangle$, (4) $\left\langle 1 - \frac{P}{N} \right\rangle$, (5) $\left\langle 1 - \frac{N}{P} \right\rangle$, (6) $\left\langle \frac{N-1}{N} - \frac{P-1}{P} \right\rangle$, (7) $\left\langle \frac{P-1}{P} - \frac{N-1}{N} \right\rangle$, (8) $\left\langle \frac{N(N-1)}{N} - \frac{P(P-1)}{P} \right\rangle$, (9) $\left\langle \frac{P(P-1)}{P} - \frac{N(N-1)}{N} \right\rangle$. Although there are many more combinations to estimate higher moments, but these are more prominent upto two particle correlations. We have calculated the higher moments of each distribution for all these quantities. The higher moment plots for these quantities are given below, calculated by the same procedure as defined above. The labels are written in terms of positive (P) and negative (N) particles.

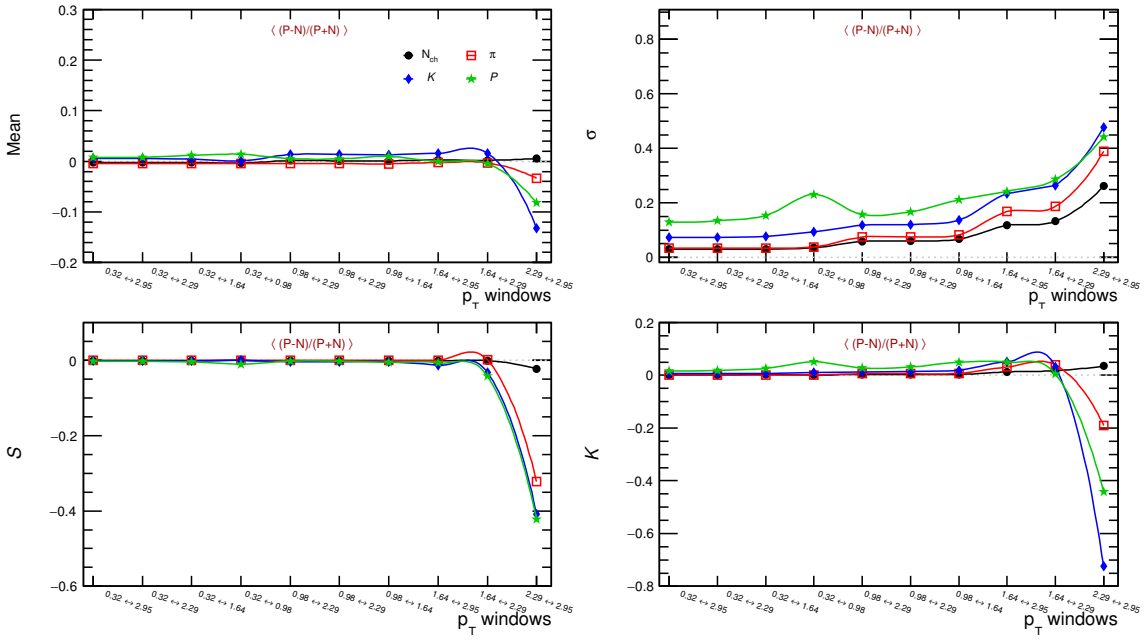

Figure 3.10: Higher moment plots for $\left\langle \frac{P-N}{P+N} \right\rangle$.

This is also for better understanding of fluctuation. All these figures shows the higher moments upto fourth order for all these combinations, for example, $\left\langle \frac{P-N}{P+N} \right\rangle$, the numerator is the net-charge and the denominator is total number of particles. The fluctuation at small p_T bin is large, because the particle content in that is very small, hence the ratio will show much fluctuation. Here also we can see the behaviour in proton and kaon system as changed from other systems. The following figures are obtained from the simulation. We observe that although the behaviour of each plot is not completely understood, but it shows a pattern of enhanced fluctuations (almost all cases) when the transverse momentum windows are reduced. It is something we are proposing from this work. If we could understand the unusual behaviour in these quantities, which are significant in the fluctuation analysis, it can give a much clear picture.

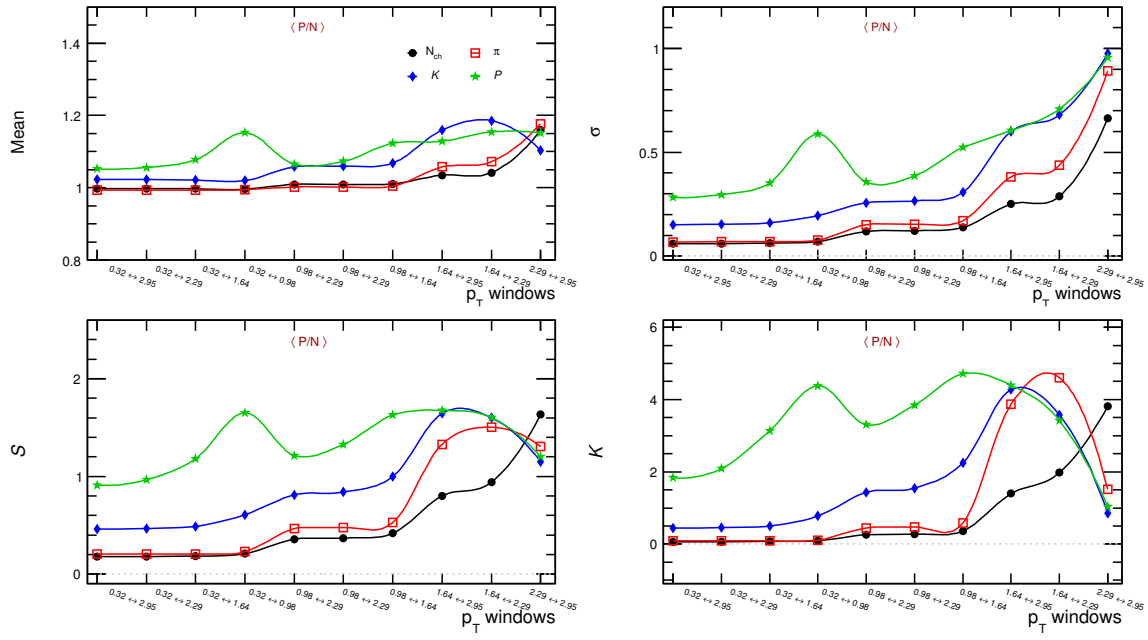

Figure 3.11: Higher moments for $\left\langle \frac{P}{N} \right\rangle$

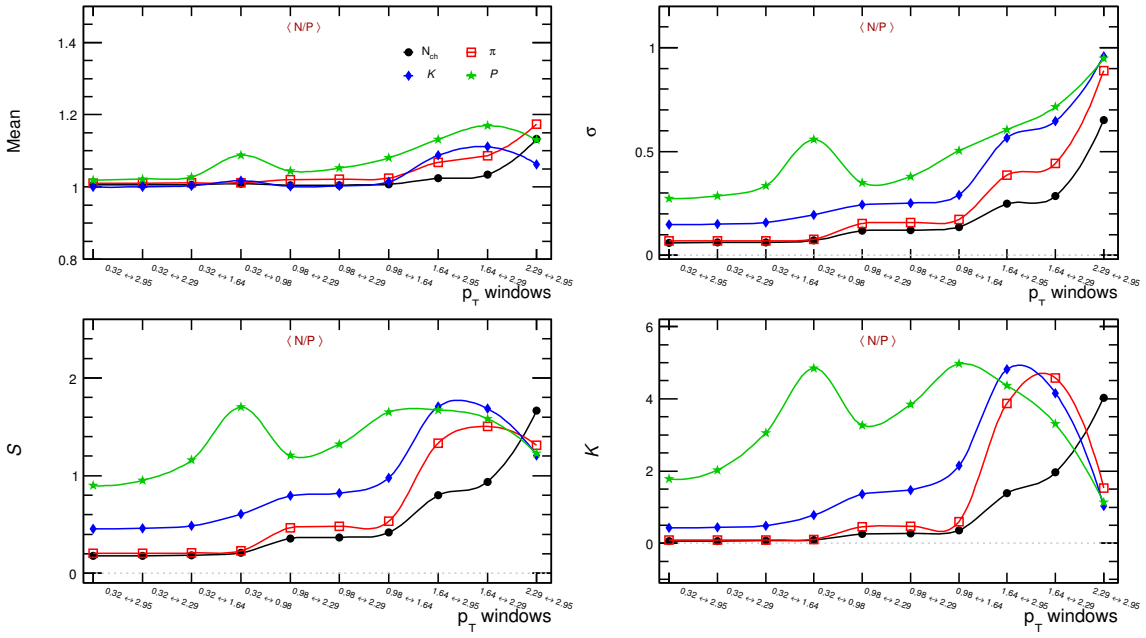

Figure 3.12: Higher moments for $\left\langle \frac{N}{P} \right\rangle$.

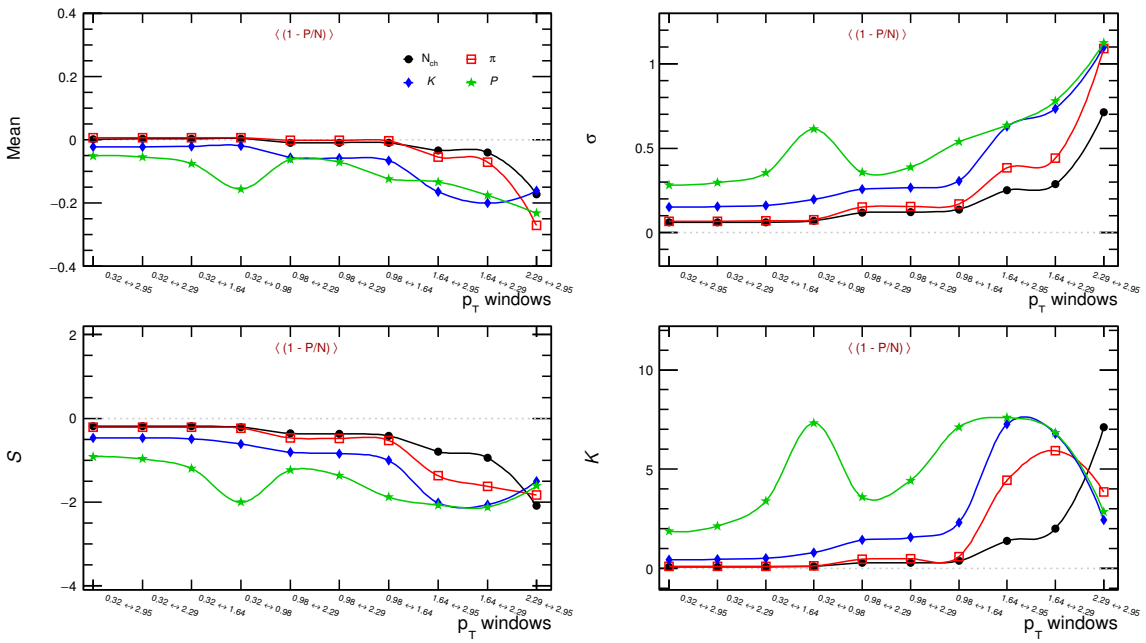

Figure 3.13: Higher moments for $\left\langle 1 - \frac{P}{N} \right\rangle$ in the event

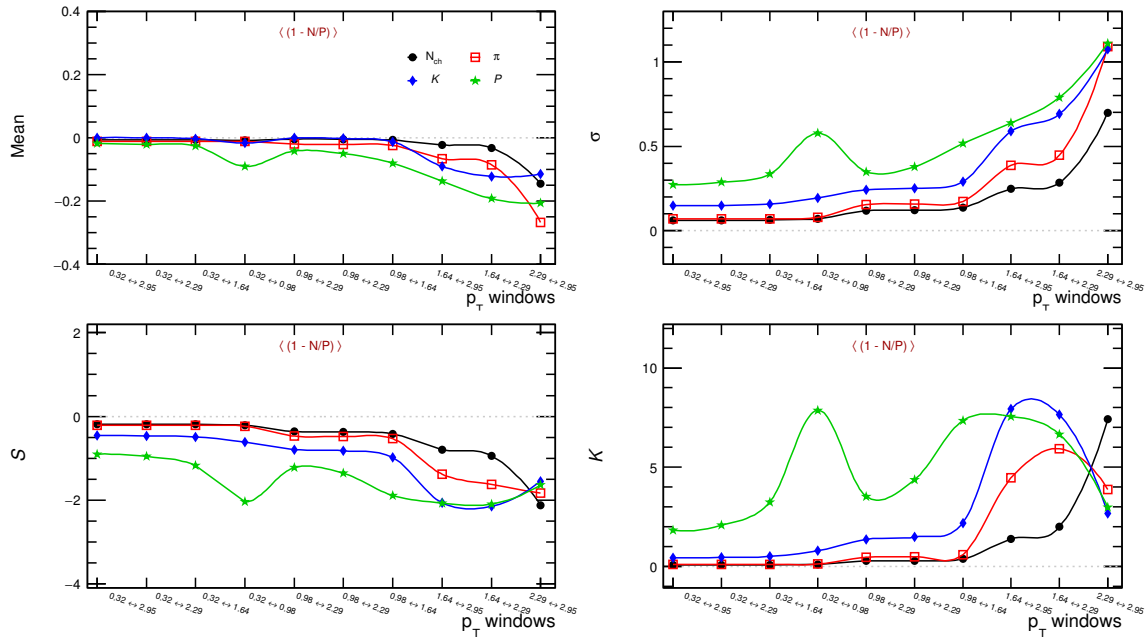

Figure 3.14: Higher moments for $\left\langle 1 - \frac{N}{P} \right\rangle$ in the event.

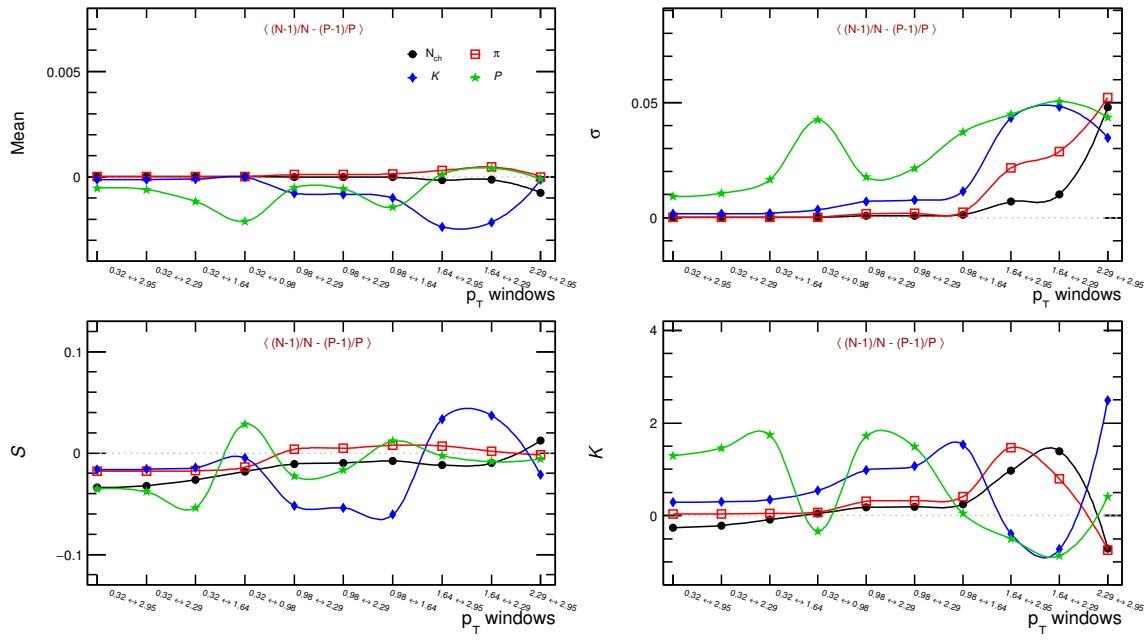

Figure 3.15: Higher moments for $\left\langle \frac{N-1}{N} - \frac{P-1}{P} \right\rangle$ in the event.

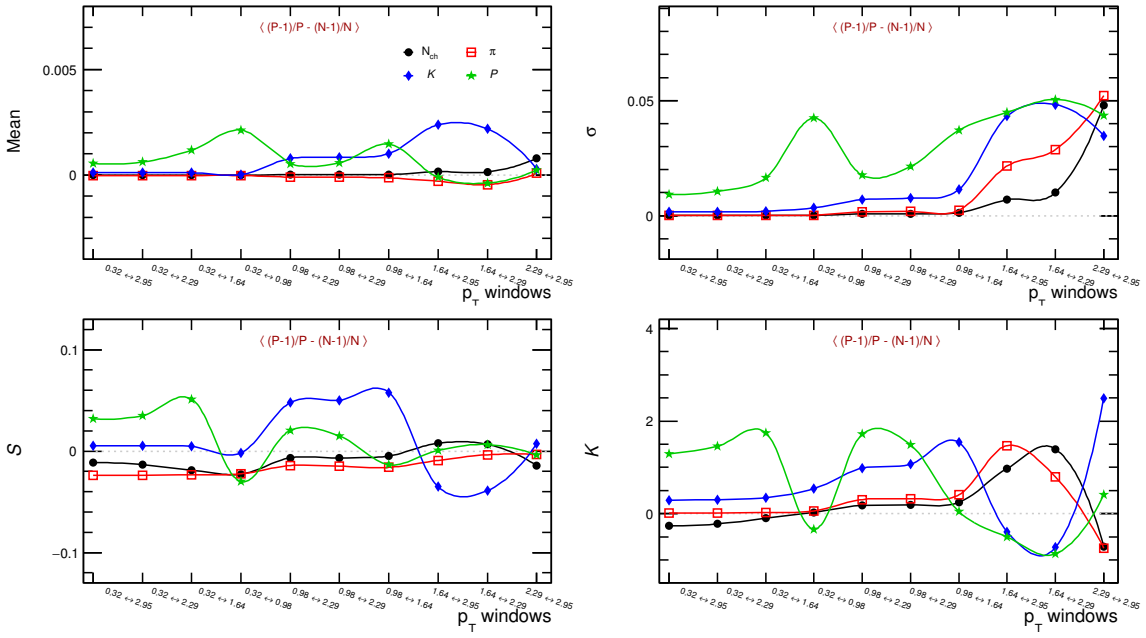

Figure 3.16: Higher moments for $\left\langle \frac{P-1}{P} - \frac{N-1}{N} \right\rangle$.

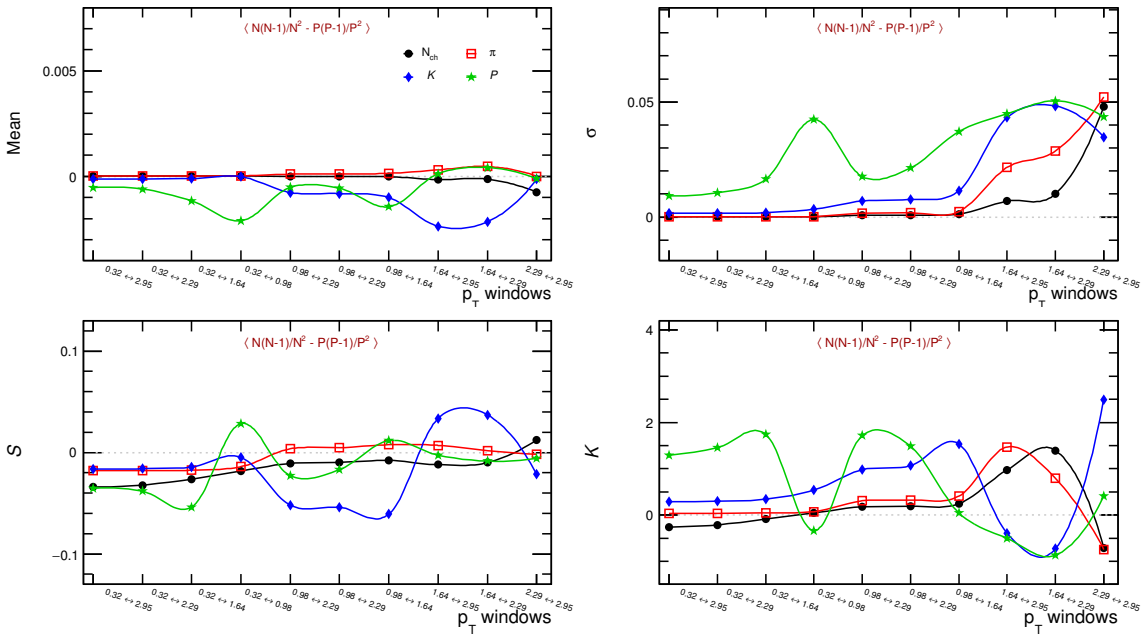

Figure 3.17: Higher moments for $\left\langle \frac{N(N-1)}{N} - \frac{P(P-1)}{P} \right\rangle$

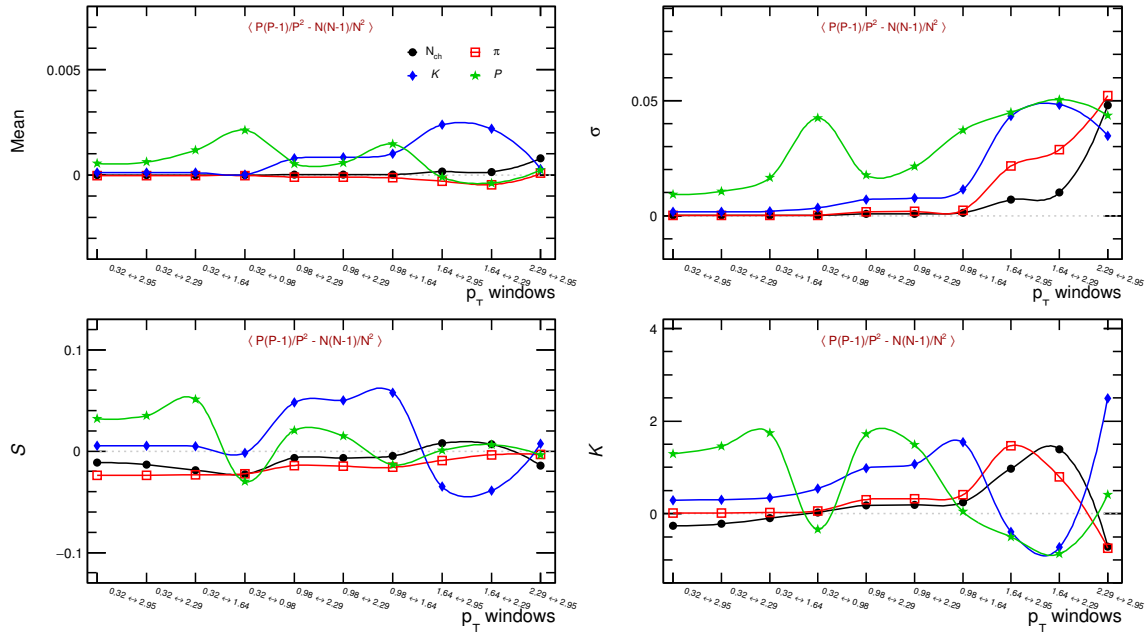

Figure 3.18: Higher moments for $\left\langle \frac{P(P-1)}{P} - \frac{N(N-1)}{N} \right\rangle$.

In summary, we can speculate that, the higher order moments for all these combinations are prominent. And it is not because of statistical fluctuations alone as we have checked with several billions of events expecting the statistical error to minimum. These quantities can be of good observables as most of them are in terms of ratios, which ensure that the partial (may be complete) cancellation of inefficiencies due to detector system in real experiments.

3.2.3 Validation of Central Limit Theorem

From section 2.1.6, the criteria for the validation of CLT is clear. In our case we need distributions with equal mean (Poisson distribution in our concern). In order to satisfy this condition, the total number of particles produced in one event has been divided into several parts, starting from two till 2700 times. For each such steps we performed Monte Carlo simulation, and produced large event size. There we carried out two different approaches, divided and flat sum approaches.

Since we are dividing the total number to, let say, n times, then the sum of these n small particle number should add up to total number which we obtained for the full integration.

For example, in the case of positive particles, the following relation should be valid.

$$P = \sum_{i=1}^{n} P_i \tag{3.1}$$

$$N = \sum_{i=1}^{n} N_i \tag{3.2}$$

where P is the total number of positive particles produced and P_i is the number of particles in each division. So, in this method we divided the total number of particles into several parts and added them. This step had done for large number of events and filled into a two dimensional histogram. The projection of this two dimensional histograms will give the expected distribution for positive and negative particles.

In figure 3.19, left panel is the two dimensional histogram for positive particle, where we are essentially checking the validity of equation 3.1. It is expected to be a band, and we are getting it nicely. The projection is the individual multiplicity distribution and it will look like right panel of figure 3.19. The colour code is used to indicate the density of points, value correspond to each colour is given at the right side of histograms. This indicator is used for the rest of the two dimensional histograms.

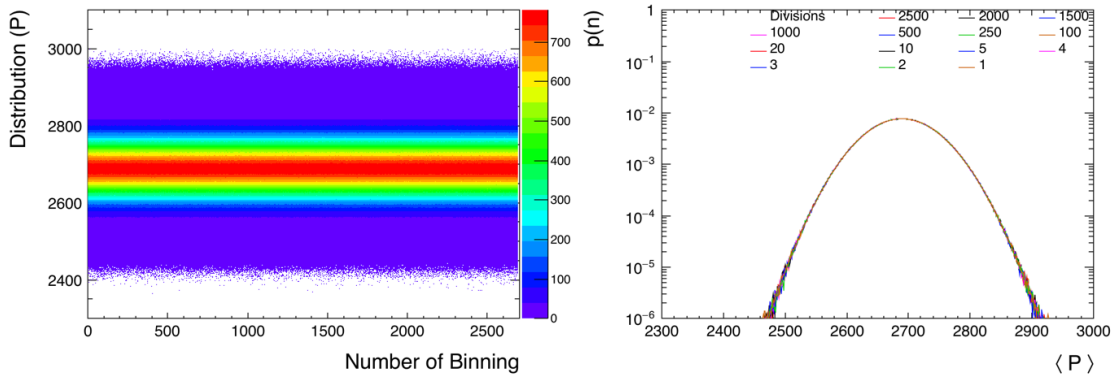

Figure 3.19: Scattered plot for positive particles simulated in various transverse momentum windows (decreasing width). Right panel is the projected distributions from each windows of scattered plot.

The two dimensional histogram for negative particles is given in the right panel of the figure 3.20. It also came as expected, a band. Individual multiplicity distribution will look like left panel of figure 3.20, corresponding to negatively charged particles.

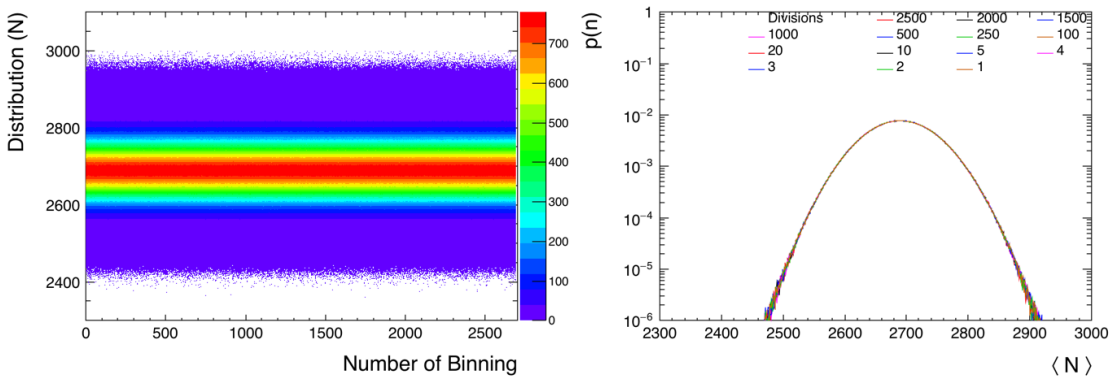

Figure 3.20: Scattered plot for negative particles simulated in various transverse momentum windows (decreasing width). Right panel is the projected distributions from each windows of scattered plot.

We can calculate the trend for net charge in this case in a similar way as we discussed for higher moment calculation of them. In each event, we have to take the difference of positive and negative particles and sum them up, fill into a two dimensional histogram. The histogram we obtained is again a band of points (right panel of figure 3.21)and its projection is given in the left panel of figure 3.21.

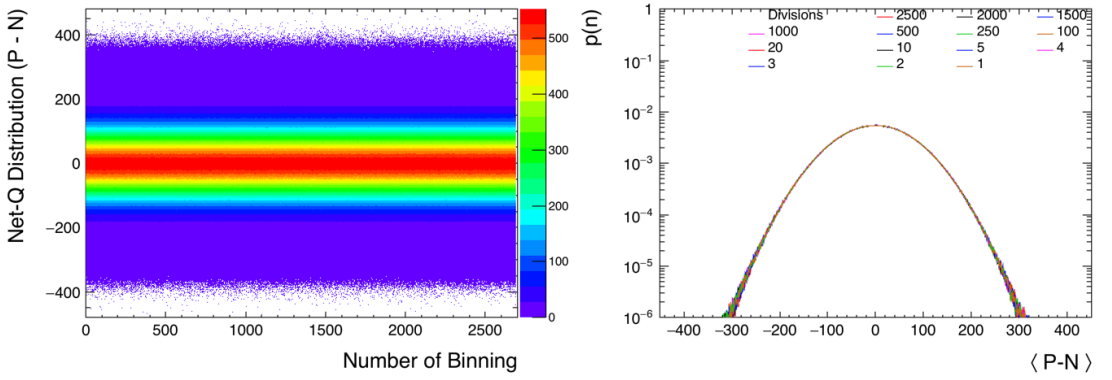

Figure 3.21: Scattered plot for net-charge simulated in various transverse momentum windows (decreasing width). Right panel is the projected distributions from each windows of scattered plot.

We need to check for another trend of these particles, when the number is not added up. This has to be checked for positive and negative particles as well as for the net-charge distribution. For positive and negative particles, we are expecting a decreasing trend,because we will get lesser number of particles in high p_T range.

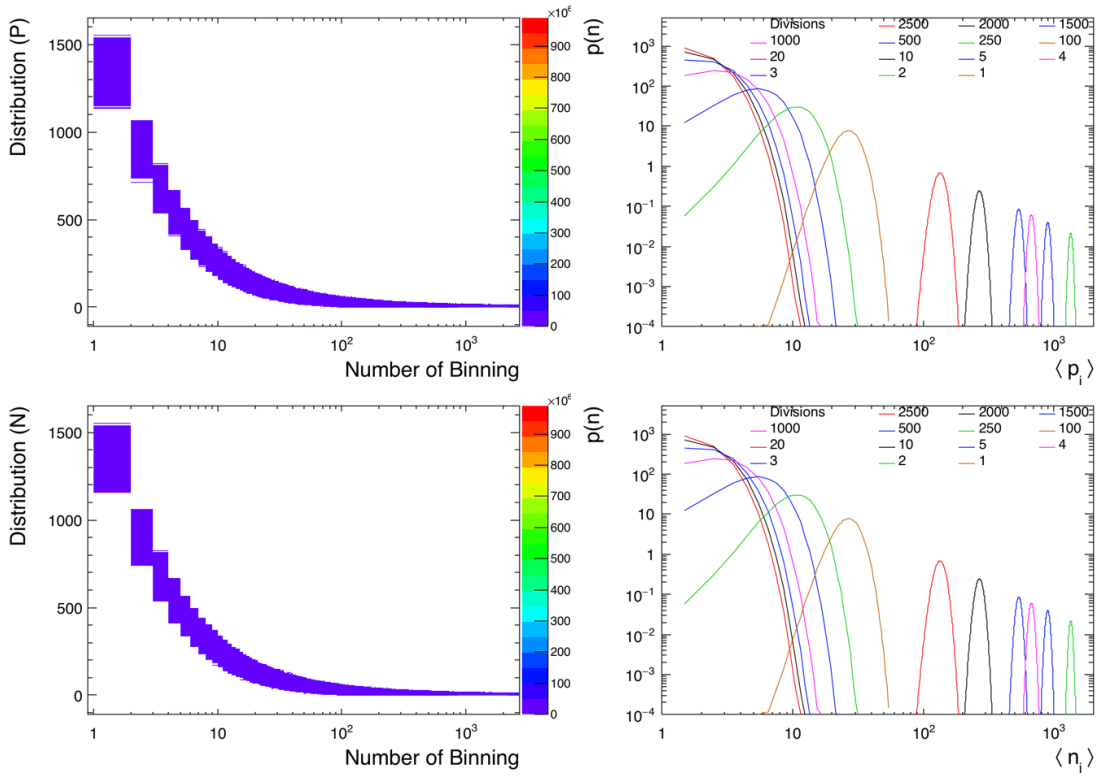

Figure 3.22: Left panels are the 2D histogram for individual divisions of positive and negative particles,from top to bottom respectively.Right panels are the projections from the scattered plots for each.

From figure 3.22, we are getting such a distribution for positive and negative particles. Left panels shows the two dimensional view of the distribution for the positive and negative particles. Right panel of figure 3.22 depicts the projections of those scattered plots in any x bin. Since it is a sum of all divisions, any projection of scattered plots will look similar.

The behaviour for positive and negative particles may not have much importance, but in the case of net- charge, it is relevant. We have to check whether the assumption we considered initially, that is the physics of conserved quantities will be same in any section of phase space, has to be checked. In this work we are looking at net-charge, it should be same in any momentum window, as per one of our initial assumption. So we need to check whether it is correct or not. We took the difference of positive and negative particles in each division and plotted.

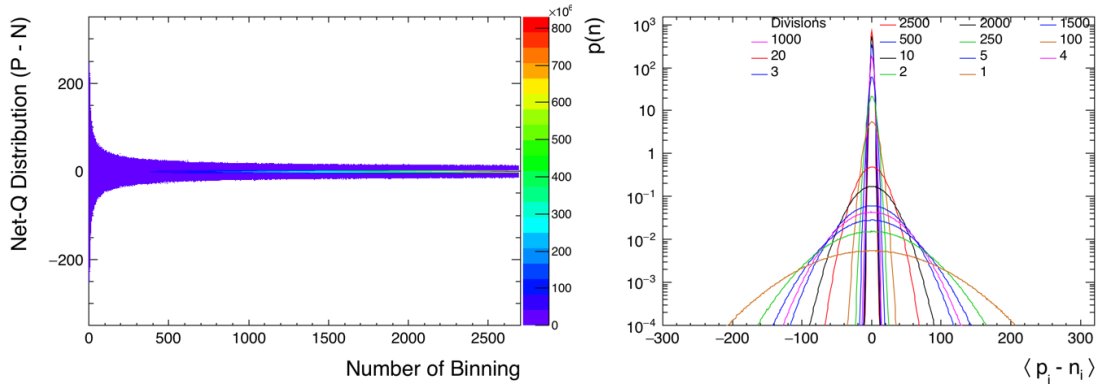

Figure 3.23: left panel is the 2D histogram for individual divisions of net-charge and right panel is the projection from the scattered plots

This result is very interesting. We are getting a converging trend as we go to higher number of division. Right panel of figure 3.23 shows the net-charge distribution as we go from total phase space to a 2700 times divided situation. It is completing the validation of central limit theorem. Because, as we are increasing the number of divisions, it is tending towards a normal distribution. So CLT is not violated. But one major assumption on which recent studies in heavy ion physics has been done, may have to reconsider. The figure 3.23 is a question towards the uniformity of phase space or more simply the physics of conserved quantities are not changing over slices of phase space. From the result we are getting, it is not the case. We can not hold that assumption for any small range of phase space, because it is changing the physics. So we need to have some normalizing conditions, in such a way that both CLT and this a prior assumption can be explained in the system. The Projection shown in the right panel will give a better understanding towards the change in the distribution as we go to higher divisions. There is less spread and more peaked around zero.

We also calculated the higher moments for these distributions of net-charge. The following plots contain the trend of higher moments for divided inputs and flat sum, both are colour coded distinctly.

From figure 3.24, it is clear that, as we go to lower number of divisions, the moments are increasing. The variance is changing very drastically compared to mean. The behaviour in figure 3.25 is also similar to above case. The conserved quantities (here, net-charge) are not showing a stable distribution as we decrease the window to very smaller.

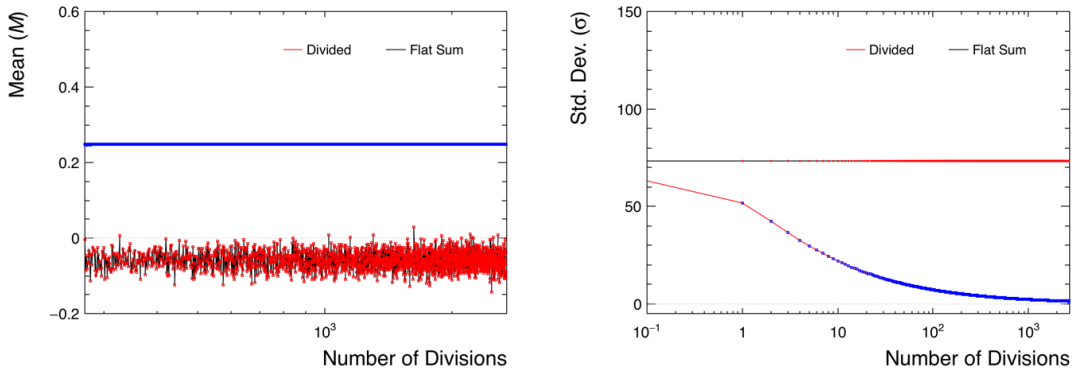

Figure 3.24: Left panel is the mean (M) and right panel is the σ of net-charge.

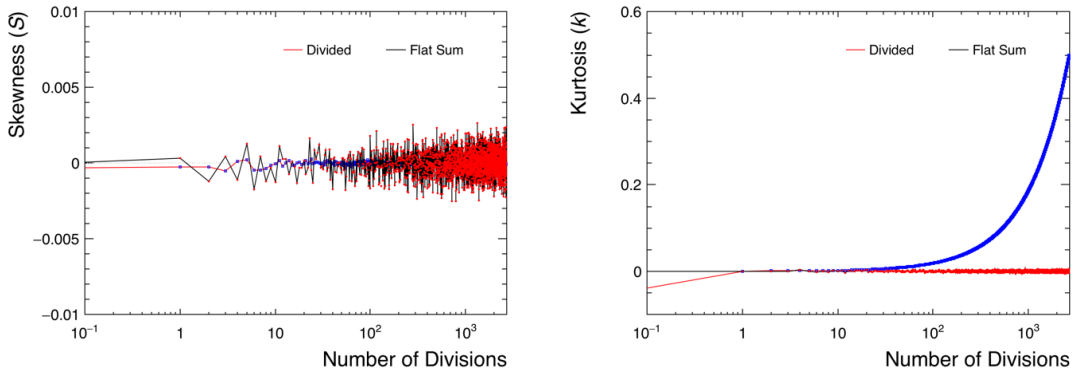

Figure 3.25: Left panel is the skewness (S) and right panel is the kurtosis (κ) of net-charge.

3.3 Summary

In tis work we mainly focused on the study of higher moments of multiplicity distributions in heavy ion collisions. Here we are briefly collating all the results and important conclusions. From various assumptions and predictions, we developed the statistical analysis method for heavy ion physics. From statistical mechanics, we got the idea to treat the system formed during collision as an ensemble, and from there the possibilities of calculating higher moments arose. We can connect the moments of the system to the susceptibility of QCD, which is related to the macroscopic parameters of QGP system. But from the equations, it was not clear that, doing such a calculation will be good for better understanding. So we did a review till second order moment (section 1.4). The findings from that study (figure 1.4) clearly showed that there is fluctuation, which is a measure of dynamical changes happening inside the system, and the study of higher moments is relevant. There we were able to see a crossover in the fluctuation as we go to higher energy regime.

In order to calculate the higher moments, we need to understand the possible distributions which can fit our multiplicity and conserved quantities. Poisson distributions can be a best candidate for multiplicity distribution at higher energy regime, while negative binomial distribution explains at lower energy regime. We are looking at ALICE data, which is an experiment at LHC, were lead atoms are colliding at higher energy. We collected data for the collision at $2.76\,TeV$ for three different particles, pions, kaons, proton and anti proton from he transverse momentum distribution. From that data, with the help of a data analysis frame work called ROOT, we were able to perform the calculation for higher moments. The result we were getting was good and it has a clear signature of fluctuation and non-zero higher moments, which is an indication of asymmetry. For representing the total system, we have done the higher moment calculation for total charged particles. Some other quantities like rations of particles, sum, ν dynamics and so on were calculated and looked into the higher moment plots of those. Those are also used previously for fluctuation studies.

The first two moments have a clear dependence on the multiplicity. From figures of the net-charge distributions for pions, kaons and protons system, the spread is decreasing. The multiplicity is also in decreasing order for these particles. The deviation in M and σ is less for protons while higher for total charged particles. Skewness and kurtosis shows a reverse correlation, because of the bias nature in the production of kaon and proton. So the fluctuations or higher moments will be large for small number of particles. Also we can see a peak at the smaller p_T bin, because, at small momentum, the number of particles will be less, and it will arise fluctuations in calculations we have done. In the validation of CLT, we got very good results. In the present situation which is developed from some a prior assumptions can not be true in full sense if CLT has to be validated. If CLT is holding then the uniform phase space concept has to redefine in such way that, using some normalizing techniques, we have to clearly mark the range up to which the uniqueness of physics, related to conserved quantities are valid. For that we have work more, it is not in the scope of this work. Also we are looking forward to do the same kind of approach in another energy scales also. Then it may help us to find some condition on the phase space slices.

Appendix A

Simulating the Events: Technical Part

We have written a set of codes using 'c++' programming language and which uses ROOT classes. Following are the main components of this monte carlo simulations.

- 1: The yields of individual particles are estimated from already published p_T spectra of each particle.
- 2: A monte-carlo event generator is written to generate both positive and negative particles.
- 3: Several parallel jobs are submitted to IISER Mohali HPC facility via a newly written qsub script
- 4: Further these outputs are collected and fed into a newly written parsing code to produce the plots.

Followings are part of several codes and scripts:

A.0.1 Simulator

```
// The integral part (x[] are the transverse momentum)
TF1 f2("f2",[&](double *x, double *){ return gr2->Eval(x[0]); },a,t,0);
double Ptotal = f2.Integral(a,b);
// Setting the Random Generator
double n;
n =(b-a)/4;
double BW[4];
```

```
for(int i=0;i<4;i++){
  BW[i] = 0.11 + n*i;
 }
TRandom *ranM[div];
TRandom *ranP[div];

for (int i = 0; i <4; i++) {
    ranM[i] = new TRandom3();
    ranP[i] = new TRandom3();
}
// Histograming
  TH2F *fHist_M[4] ;
  TH2F *fHist_Q[4] ;
  TH2F *fHist_P[4] ;
// Generating events
for(int j=1; j<=z ;j++){
  ranM[j-1]->SetSeed(0);
  ranP[j-1]->SetSeed(0);
  double al = BW[i] ;
  double au = BW[i] + n*j;
  double yieldP = f2.Integral(al,au);
  double yieldM = f1.Integral(al,au);
  for(int k=0; k<nevt;k++){
    m = ranM[j-1]->Poisson(yieldM);
    p = ranP[j-1]->Poisson(yieldP);
    q = p-m;
     .....
     .....
     .....
}
```

A.0.2 Simulator for CLT

```
// Generating CLT Events
TRandom *ranM[div];
TRandom *ranP[div];

for (int i = 0; i <div; i++) {
    ranM[i] = new TRandom3();
```

```
7       ranP[i] = new TRandom3();
8       ranM[i]->SetSeed(0);
9       ranP[i]->SetSeed(0);
10  }
11  .....
12  .....
13  double sumM, a10 = 0;
14  double sumP, a11 = 0;
15  for(int i=1;i<= div;i++){
16          double meanP = Ptotal/i ;
17          double meanM = Mtotal/i ;
18          Printf("Running For: %d P:%f N:%f", i, meanP, meanM);
19          for(int k=0;k<nevt;k++){
20                  sumP = 0;
21                  sumM = 0;
22                  for(int j=0;j<i;j++){
23                   a10 = ranM[j]->Poisson(meanP);
24                   a11 = ranP[j]->Poisson(meanM);
25
26                   sumP += a10;
27                   sumM += a11;
28
29                   fHist_iP->Fill(i-1,a10);
30                   fHist_iM->Fill(i-1,a11);
31                   fHist_iQ->Fill(i-1,(a10-a11));
32                  }
33                  double Q = sumP - sumM;
34                  fHist_P->Fill(i-1,sumP);
35                  fHist_M->Fill(i-1,sumM);
36                  fHist_Q->Fill(i-1,Q);
37
38          }
39  }
```

A.0.3 qsub script

```
1  #!/bin/bash
2  ################################
3  # Example to use /tmp space - qsub script
```

```
# Written for IISER HPC community
# Author: S. Jena
# Sat Mar  4 14:23:52 IST 2017
#################################
#
###### BEGIN SGE PARAMETERS - note the '#$' prefix ######
###### DO NOT SET THE -cwd flag for a /tmp job
#
#$ -S /bin/bash
# specify the name of the job displayed in 'qstat' output
#$ -N anjali
#
######## Where to keep Log Output #########
# Make sure you have  a directory log in your HOME
#$ -o log/
#$ -e log/
###### BEGIN  /tmp DIR CODE  ######
# set the STDATA to point to the node-local /tmp dir and make sure you
# place the files in your own subdir. '${USER}' is global environment
# variable inherited by all your processes, so you shouldn't have to
# define it explicitly
#JOB_ID get the job number and we keep output in folder with this number
COPUT="HM${JOB_ID}"
STDATA="/tmp/${USER}/${COPUT}"
MYAPP="${HOME}/hm/run.sh"
FOUTPUTD="${HOME}/hm/output"
mkdir -p ${STDATA}
mkdir -p ${FOUTPUTD}
cd ${STDATA}
cd ${STDATA}
pwd
cp ${HOME}/hm/run.sh .
cp ${HOME}/hm/CLTupdated.C .
cp ${HOME}/hm/produceHistForHM.C .
pwd
sh run.sh
rm *.C *.sh *.pcm *.so *.d
cd ../
cp -r ${COPUT} ${FOUTPUTD}/.
```

```
rm -rf ${COPUT}
```

A.0.4 Run Script

```
#!/bin/sh
#source /opt/cern/root/bin/thisroot.sh
#export PATH=$PATH:/opt/cern/root/bin
#export LD_LIBRARY_PATH=$LD_LIBRARY_PATH:/opt/cern/root/lib/root
#module avail
module load cern/1
root -b << EOF
.L produceHistForHM.C+
produceHistForHM()
.q
EOF
for i in {0..50}
do
    root -b -q 'CLTupdated.C('${i}')' 2>&1 | tee check_${i}.log
done
hadd OutputHistCLT.root cltoutput*.root
rm cltoutput*.root
```

A.0.5 Submitting Job and Logs

We submit job using SGE job scheduler and it was done via following commands

```
[fontsize=\small]
#qsub run_job.qsub
Your job 17354 ("anjali") has been submitted
```

We submit several such jobs to achieve the statistics. Once jobs are submitted, it pass to the computing nodes.

```
#qstat
job-ID prior  name  user  state submit/start at   queue  slots/ja-task-ID
-----------------------------------------------------------------------------
16754 0.55500 anjali sjena  r   04/16/2017 11:06:52 all.q@compute-0-3  1
16755 0.55500 anjali sjena  r   04/16/2017 11:06:52 all.q@compute-0-14 1
16756 0.55500 anjali sjena  r   04/16/2017 11:06:52 all.q@compute-0-13 1
16757 0.55500 anjali sjena  r   04/16/2017 11:06:52 all.q@compute-0-12 1
```

```
16758 0.55500 anjali sjena  r   04/16/2017 11:06:52 all.q@compute-0-6  1
16759 0.55500 anjali sjena  r   04/16/2017 11:06:52 all.q@compute-0-16 1
16760 0.55500 anjali sjena  r   04/16/2017 11:06:52 all.q@compute-0-9  1
16761 0.55500 anjali sjena  r   04/16/2017 11:06:52 all.q@compute-0-11 1
16762 0.55500 anjali sjena  r   04/16/2017 11:06:52 all.q@compute-0-5  1
16763 0.55500 anjali sjena  r   04/16/2017 11:06:52 all.q@compute-0-4  1
16764 0.55500 anjali sjena  r   04/16/2017 11:06:52 all.q@compute-0-7  1
16765 0.55500 anjali sjena  r   04/16/2017 11:06:52 all.q@compute-0-7  1
16766 0.55500 anjali sjena  r   04/16/2017 11:06:52 all.q@compute-0-4  1
16767 0.55500 anjali sjena  r   04/16/2017 11:06:52 all.q@compute-0-5  1
$qstat -f  (tells about slots and number of jobs)
queuename        qtype resv/used/tot. load_avg arch          states
---------------------------------------------------------------------
all.q@compute-0-0.local  BIP   0/12/12        12.01    linux-x64
  16823 0.55500 anjali  sjena    r     04/16/2017 11:06:52     1
  16842 0.55500 anjali  sjena    r     04/16/2017 11:06:52     1
  16861 0.55500 anjali  sjena    r     04/16/2017 11:06:52     1
  16880 0.55500 anjali  sjena    r     04/16/2017 11:06:52     1
  16899 0.55500 anjali  sjena    r     04/16/2017 11:06:52     1
  16918 0.55500 anjali  sjena    r     04/16/2017 11:06:52     1
  16937 0.55500 anjali  sjena    r     04/16/2017 11:06:52     1
  16955 0.55500 anjali  sjena    r     04/16/2017 11:12:07     1
  16960 0.55500 anjali  sjena    r     04/16/2017 11:12:07     1
  16966 0.55500 anjali  sjena    r     04/16/2017 11:12:07     1
  16970 0.55500 anjali  sjena    r     04/16/2017 14:26:07     1
  16978 0.55500 anjali  sjena    r     04/16/2017 15:04:07     1
```

This produces two log files 'anjali.e16981' and 'anjali.o16981', which keep all the 'stdout' of the ROOT simulator that is running.

```
[fontsize=\small]
/tmp/HM16981
/tmp/HM16981
------------------------------------------------------------
| Welcome to ROOT 6.02/05              http://root.cern.ch |
```

```
|                                (c) 1995-2014, The ROOT Team |
| Built for linuxx8664gcc                                     |
| From tag v6-02-05, 9 February 2015                          |
| Try'.help', '.demo','.license', '.credits', '.quit'/'.q'    |
-------------------------------------------------------------
Processing CLTupdated.C(0)...
Info in <TCanvas::MakeDefCanvas>:  created default
TCanvas with name c1
p=2689.563987 m=2690.121991
Running For: 1 P:2689.563987 N:2690.121991
Running For: 2 P:1344.781993 N:1345.060995
```

A.0.6 Analysis and output Parsing Code

```
ivoid mySetGraphStyle();
void myGraphSetUp( TGraphErrors *currentGraph=0,
                   Float_t currentMarkerSize = 1.0,
                   int currentMarkerStyle=20,
                   int currentMarkerColor=0,
                   int currentLineStyle=1,
                   int currentLineColor=0);
void myPadSetUp(   TPad *currentPad,
                   float currentLeft=0.11,
                   float currentTop=0.04,
                   float currentRight=0.04,
                   float currentBottom=0.15);
void myLegendSetUp(TLegend *currentLegend=0,
                   float currentTextSize=0.07);
//-----------------------------------------------
void DrawProjHisto1Can(TH2F* vHist,
                       const Char_t *figname,
                       const Char_t *strXaxis,
                       const Char_t *strYaxis,
                       Char_t *strLeg[kNpt]);

//-----------------------------------------------
void DrawGraph1Can4Pad(TH2F *lHist, Int_t type, const Char_t *figname);
```

```
.....
.....
TFile *file = TFile::Open("OutputHistHM.root");
TH2F* fHist[4][13];
for(Int_t iPid = 0; iPid < 4; iPid++) {
    for(Int_t iPhy = 0; iPhy < 13; iPhy++) {
      fHist[iPid][iPhy] = (TH2F*)file->Get(Form("%s%d", hname[iPhy],
    iPid));
      cout << fHist[iPid][iPhy]->GetName() << endl;
    }
}
....
DrawProjHisto1Can(fHistClone[0][0], "figDistChargeP", "#LT P #GT", "p(n)
    ", strLeg);
....
for (Int_t i = 0; i < lHist->GetNbinsX(); i++) {
    TH1D *htmp = (TH1D*)lHist->ProjectionY(Form("_Phist%s%d",lHist->
    GetName(),i), i+1, i+1,"");
    xa[i] = i;
    me[i] = htmp->GetMean(); mee[i] = htmp->GetMeanError();
    si[i] = htmp->GetRMS();  sie[i] = htmp->GetRMSError();
    sk[i] = htmp->GetSkewness();
    ku[i] = htmp->GetKurtosis();
}
...
...
TGraphErrors *gr_me = new TGraphErrors(kNpt, xa, me, 0, mee);
TGraphErrors *gr_si = new TGraphErrors(kNpt, xa, si, 0, sie);
TGraphErrors *gr_sk = new TGraphErrors(kNpt, xa, sk, 0, 0);
TGraphErrors *gr_ku = new TGraphErrors(kNpt, xa, ku, 0, 0);
....
 TCanvas *myCan = new TCanvas(Form("myCan_%s",figname),"",960,700);
  myCan->Draw();
....
gr_me->Draw("SAME CP");
gr_si->Draw("SAME CP");
gr_sk->Draw("SAME CP");
gr_ku->Draw("SAME CP");
```

```
// Analyzing and drawing CLT
void Draw2Dhisto(  const Char_t *figname,
                   TH2* h,
                   const Char_t *strXaxis,
                   const Char_t *strYaxis);
void DrawProjHisto(const Char_t *figname,
                   const Int_t nHist,
                   TH1D* vHist[nHist],
                   const Char_t *strXaxis,
                   const Char_t *strYaxis,
                   const Char_t *strLeg[nHist]);

void DrawGraphComp(const Char_t *figname,
                   const Int_t ngr,
                   TGraphErrors *gr[ngr],
                   const Char_t *strXaxis,
                   const Char_t *strYaxis,
                   const Char_t *strLeg[ngr]);
....
....
 TFile *file = TFile::Open("fullstat/OutputHistCLT.root");
  // Reading all Histograms
  TH2F  *fHist_PC  = (TH2F*)file->Get("fHist_P");
  TH2F  *fHist_MC  = (TH2F*)file->Get("fHist_M");
  TH2F  *fHist_QC  = (TH2F*)file->Get("fHist_Q");
  TH2F  *fHist_iPC = (TH2F*)file->Get("fHist_iP");
  TH2F  *fHist_iMC = (TH2F*)file->Get("fHist_iM");
  TH2F  *fHist_iQC = (TH2F*)file->Get("fHist_iQ");
...
...
 Draw2Dhisto("Plus", fHist_PC, "Number of Binning", "Distribution (P)");
    Draw2Dhisto("Minus", fHist_MC, "Number of Binning", "Distribution (N
   )");
....
 for (Int_t i = 0; i < nbin; i++) {
      fhistP[i]   = (TH1D*)fHist_P->ProjectionY(Form("_Phist%d",binpos[i
   ]), binpos[i], binpos[i],"");
      fhistN[i]   = (TH1D*)fHist_M->ProjectionY(Form("_Nhist%d",binpos[i
   ]), binpos[i], binpos[i],"");
```

```
37        fhistQ[i]    = (TH1D*)fHist_Q->ProjectionY(Form("_Qhist%d",binpos[i
      ]), binpos[i], binpos[i],"");
38        fhistInP[i] = (TH1D*)fHist_iP->ProjectionY(Form("_iPhist%d",binpos
      [i]), binpos[i], binpos[i],"");
39        fhistInN[i] = (TH1D*)fHist_iM->ProjectionY(Form("_iNhist%d",binpos
      [i]), binpos[i], binpos[i],"");
40        fhistInQ[i] = (TH1D*)fHist_iQ->ProjectionY(Form("_iQhist%d",binpos
      [i]), binpos[i], binpos[i],"");
41        fhistInQ[i]->Rebin(2,"");
42     }
43 .....
44 DrawProjHisto("DistP", nbin, fhistP, "#LT P #GT", "p(n)", strLeg);
45 DrawProjHisto("DistN", nbin, fhistN, "#LT N #GT", "p(n)", strLeg);
46 ....
47 // Similar functions line HM analysis are being used to draw the results
      .
```

Bibliography

[A+02] M. M. Aggarwal et al., *Event-by-event fluctuations in particle multiplicities and transverse energy produced in 158-A-GeV Pb + Pb collisions*, Phys. Rev. **C65** (2002), 054912.

[A+09] B. I. Abelev et al., *K/pi Fluctuations at Relativistic Energies*, Phys. Rev. Lett. **103** (2009), 092301.

[A+13] Betty Abelev et al., *Net-Charge Fluctuations in Pb-Pb collisions at* $\sqrt{s}_{NN} = 2.76$ *TeV*, Phys. Rev. Lett. **110** (2013), no. 15, 152301.

[A+14] Betty Bezverkhny Abelev et al., *Production of charged pions, kaons and protons at large transverse momenta in pp and Pb–Pb collisions at* $\sqrt{s_{\rm NN}}$ *=2.76 TeV*, Phys. Lett. **B736** (2014), 196–207.

[A+15] N. M. Abdelwahab et al., *Energy Dependence of* K/π*,* p/π*, and* K/p *Fluctuations in Au+Au Collisions from* $\sqrt{\rm s_{NN}}$ *= 7.7 to 200 GeV*, Phys. Rev. **C92** (2015), no. 2, 021901.

[ABMRS17] A. Andronic, P. Braun-Munzinger, K. Redlich, and J. Stachel, *Hadron yields, the chemical freeze-out and the QCD phase diagram*, J. Phys. Conf. Ser. **779** (2017), no. 1, 012012.

[ALI] *Linear accelerator 3*, https://home.cern/about/accelerators/linear-accelerator-3.

[Ars16] Mesut Arslandok, *Event-by-Event Identified Particle Ratio Fluctuations in Pb–Pb Collisions with ALICE using the Identity Method*, Nucl. Phys. **A956** (2016), 870–873.

[BBC+90] Frank R. Brown, Frank P. Butler, Hong Chen, Norman H. Christ, Zhi-hua Dong, Wendy Schaffer, Leo I. Unger, and Alessandro Vaccarino, *On the existence of a phase transition for QCD with three light quarks*, Phys. Rev. Lett. **65** (1990), 2491–2494.

[BMFK+12] P. Braun-Munzinger, B. Friman, F. Karsch, K. Redlich, and V. Skokov, *Net-charge probability distributions in heavy ion collisions at chemical freeze-out*, Nucl. Phys. **A880** (2012), 48–64.

[Cha14] A. K. Chaudhuri, *A short course on Relativistic Heavy Ion Collisions*, IOPP, 2014.

[CHS09] P. Christiansen, E. Haslum, and E. Stenlund, *Number-ratio fluctuations in high-energy particle production*, Phys. Rev. **C80** (2009), 034903.

[Eji08] Shinji Ejiri, *Canonical partition function and finite density phase transition in lattice QCD*, Phys. Rev. **D78** (2008), 074507.

[Hei01] Henning Heiselberg, *Event-by-event physics in relativistic heavy ion collisions*, Phys. Rept. **351** (2001), 161–194.

[JHZ16] Zhi-Jin Jiang, Jia-Qi Hui, and Yu Zhang, *The rapidity and thermal motion induced transverse momentum distributions of identified charged particles produced in Au-Au collisions at RHIC energies*.

[M07] Kardar M, *Statistical physics of fields*, Cambridge University Press, 2007.

[O+14] K. A. Olive et al., *Review of Particle Physics*, Chin. Phys. **C38** (2014), 090001.

[Oer06] R. Oerter, *The theory of almost everything: The standard model, the unsung triumph of modern physics*, 2006.

[PGV02] C. Pruneau, S. Gavin, and S. Voloshin, *Methods for the study of particle production fluctuations*, Phys. Rev. **C66** (2002), 044904.

[Poi] *Poisson distributions - properties, normal distributions- properties. theoretical distributions. discrete distribution*, http://docplayer.net/30271755-

Lecture-7-poisson-distributions-properties-normal-distributions-properties-theoretical-distributions-discrete-distribution.html.

[RHI] *The physics of rhic*, https://www.bnl.gov/rhic/physics.asp.

[ROO] *Root reference documentation*, https://root.cern.ch/root/html606/.

[Ros07] Sheldon M Ross, *A first course in probability*, Pearson, 2007.

[Sal09] C A Salgado, *Lectures on high-energy heavy-ion collisions at the LHC*, 42 p.

[Sat11] Helmut Satz, *The Quark-Gluon Plasma: A Short Introduction*, Nucl. Phys. **A862-863** (2011), 4–12.

[SRS99] Misha A. Stephanov, K. Rajagopal, and Edward V. Shuryak, *Event-by-event fluctuations in heavy ion collisions and the QCD critical point*, Phys. Rev. **D60** (1999), 114028.

[Taw13] A. Tawfik, *On the Higher Moments of Particle Multiplicity, Chemical Freeze-Out and QCD Critical Endpoint*, Adv. High Energy Phys. **2013** (2013), 574871.

[TW13] Terence J. Tarnowsky and Gary D. Westfall, *First Study of the Negative Binomial Distribution Applied to Higher Moments of Net-charge and Net-proton Multiplicity Distributions*, Phys. Lett. **B724** (2013), 51–55.

[wik] *Relativistic heavy ion collider*, $https://en.wikipedia.org/wiki/Relativistic_Heavy_Ion_Collider$.